Simulating oxygen isotope ratios in tree ring cellulose using a dynamic global vegetation model

S. G. Keel[1*], F. Joos[1], R. Spahni[1], M. Saurer[2], R. B. Weigt[2], S. Klesse[3,4]

[1]{University of Bern, Physics Institute, Climate and Environmental Physics & Oeschger Centre for Climate Change Research, Bern, Switzerland}

[2]{Paul Scherrer Institute, Laboratory of Atmospheric Chemistry, Villigen, Switzerland}

[3] {Swiss Federal Research Institute WSL, Birmensdorf, Switzerland}

[4] {Oeschger Centre for Climate Change Research, Bern, Switzerland}

[*]{now at: Agroscope, Institute for Sustainability Sciences, Climate and Air Pollution, Zurich, Switzerland}

Correspondence to: S. G. Keel (sonja.keel@agroscope.admin.com)

Abstract

Records of stable oxygen isotope ratios in tree rings are valuable tools to reconstruct past climatic conditions and the response of trees to those conditions. So far the use of stable oxygen isotope signatures of tree rings has not been systematically evaluated in dynamic global vegetation models (DGVMs). DGVMs integrate many hydrological and physiological processes and their application could improve proxy-model comparisons and the interpretation of oxygen isotope records. Here we present an approach to simulate leaf water and stem cellulose δ^{18}O of trees using the LPX-Bern DGVM (LPX-Bern). Our results lie within a few per mil of measured tree ring δ^{18}O of thirty-one different forest stands mainly located in Europe. Temporal means over the last five decades as well as inter-annual variations for a subset of sites in Switzerland are captured. A sensitivity analysis reveals that relative humidity, temperature, and the water isotope boundary conditions have the largest influence on simulated stem cellulose δ^{18}O, followed by all climatic factors combined, whereas increasing atmospheric CO_2 and nitrogen deposition exert no

36 impact. We conclude that simulations with LPX-Bern are useful to investigate large-scale oxygen

37 isotope patterns of tree-ring cellulose, to elucidate the importance of different environmental

38 factors on isotope variations and therefore help to reduce uncertainties in the interpretation of

39 $\delta^{18}O$ of tree-rings.

40

41 **1   Introduction**

42 Stable oxygen isotope ratios ($^{18}O/^{16}O$) are widely used to reconstruct past climatic conditions and

43 to characterize the modern hydrological cycle. $\delta^{18}O$ ($\delta^{18}O$ =[(($^{18}O/^{16}O)_{sample}/(^{18}O/^{16}O)_{standard}$)-

44 1]$*$1000 [‰]) is routinely measured in various climate archives such as ice cores (Dansgaard,

45 1964; Johnsen et al., 2001; Jouzel et al., 2003; Severinghaus et al., 2009), speleothems

46 (Fleitmann et al., 2004; McDermott, 2004), corals (Dunbar et al., 1994), ocean sediments

47 (Shackleton and Obdyke, 1973; Elderfield and Ganssen, 2000), and tree rings (Libby et al., 1976;

48 Treydte et al., 2006) as well as in modern precipitation samples (Rozanski et al., 1992; Kern et

49 al., 2014). Regarding the tree ring archive, recent efforts were directed to document $\delta^{18}O$

50 variability in stem cellulose from tree ring samples over the last millennium (e.g. Masson-

51 Delmotte et al., 2005; Treydte et al., 2006; Edwards et al., 2008) and the industrial period

52 (Anderson et al., 1998; Miller et al., 2006). The spatial distribution of tree ring $\delta^{18}O$ has been

53 characterized across large areas (e.g. Saurer et al., 2002; Herweijer et al., 2007; Treydte et al.,

54 2007). In addition, attempts have been made to unravel the processes that determine stem

55 cellulose $\delta^{18}O$ (e.g. Gessler et al., 2009; Offermann et al., 2011).

56 The cycling of water isotopes through the climate system including the transfer of water

57 associated with gross primary productivity on land was successfully implemented in atmospheric

58 general circulation and in Earth System Models (Joussaume et al., 1984; Jouzel et al., 1987;

59 Hoffmann et al., 1998; Noone and Simmonds, 2002; Sturm et al., 2005; Werner et al., 2011) to

60 characterize the hydrological cycle. Model results are used to demonstrate that the El Niño

61 Southern Oscillation imprints a pronounced signal on water isotopes (Hoffmann et al. 1998), to

62 reconstruct past precipitation patterns (Risi et al., 2010; Sjolte et al., 2011; Masson-Delmotte et

63 al., 2015), and to explain $\delta^{18}O$ paleo data (Hoffmann et al., 2003). Model results are evaluated

64 against stable isotope ratios in precipitation (Joussaume et al., 1984), snow (Jouzel et al., 1987),

2

65 ground water (Hoffmann et al., 1998), water vapor (Werner et al., 2011), and ice core $\delta^{18}O$ data

66 (e.g. Risi et al., 2010). Because none of these models describes $\delta^{18}O$ in stem cellulose, a direct

67 model-data comparison is not yet possible for tree rings and global scale models. So far process

68 models describing the transfer of isotopic signals from soil water and water vapor to leaf water,

69 and finally stem cellulose, were applied for single sites only (Roden et al., 2000; Ogée et al. 2009;

70 Kahmen et al., 2011; Treydte et al., 2014). Yet, the implementation of such an approach in large-

71 scale global land biosphere models is missing. A large-scale approach would have the advantage

72 that many hydrological and physiological processes could be integrated and large spatial and

73 temporal patterns could be explored. Furthermore the importance of individual factors such as

74 rising atmospheric CO_2 could easily be examined.

75 The goals of this study are (i) to describe the implementation of the stable water isotope fluxes

76 and pools in the LPX-Bern DGVM, including $\delta^{18}O$ in stem cellulose for direct model-proxy

77 comparison, (ii) to estimate the large-scale spatial distribution of $\delta^{18}O$ in leaf water and stem

78 cellulose, (iii) to quantify the drivers of spatio-temporal trends and variability of stem cellulose

79 $\delta^{18}O$ in the model context and to assist in the interpretation of tree ring $\delta^{18}O$ data, and (iv) to

80 assess the model performance for large-scale spatial gradients, multi-decadal trends, and inter-

81 annual variability with a focus on extra-tropical forests. We compiled time-averaged tree ring

82 $\delta^{18}O$ data from thirty-one boreal and temperate forest sites to capture spatial variability and use

83 five tree-ring-$\delta^{18}O$ records from Switzerland to detail local temporal variability. Soil water and

84 water vapor $\delta^{18}O$ results from transient simulations with the model ECHAM5-JSBACH (Haese et

85 al., 2013) over the past 50 years are used as oxygen isotope input data (i.e. isotope forcing).

86 Factorial experiments at the site scale are performed to identify drivers of decadal trends and

87 inter-annual variability.

1.1 Isotope background

89 Evaporation and condensation are the two processes that predominantly influence water oxygen

90 isotope ratios in the climate system. Water molecules containing the lighter ^{16}O isotopes

91 evaporate more readily compared to molecules containing the heavier ^{18}O. Therefore moisture

92 evaporated from the ocean is depleted in ^{18}O compared to ocean water, which has a $\delta^{18}O$ of near

93 zero per mil. As air cools by rising into the atmosphere or moving toward the poles, moisture

Sonja Keel 3/2/2016 8:27 PM
Deleted: -

Sonja Keel 4/1/2016 9:52 AM
Deleted: Dynamic Global Vegetation Model (
Sonja Keel 4/1/2016 9:52 AM
Deleted:)

Sonja Keel 3/29/2016 9:47 AM
Deleted: applied as boundary conditions

3

98   begins to condense and falls as precipitation. Water vapor molecules containing ^{18}O condense
99   more readily and rain is enriched in ^{18}O compared to its vapor source. As the air continues to
100   move pole-ward into colder regions (temperature effect) or further inland (continental effect) the
101   remaining moisture in the air as well as the water that condenses and precipitates become
102   increasingly more ^{18}O depleted. This is reflected in the spatial distribution of oxygen isotope
103   ratios in soil water and water vapor. The $\delta^{18}O$ of surface soil water reflects the $\delta^{18}O$ signal of
104   precipitation averaged over a certain amount of time and is further modified by evaporation of
105   soil water leading to evaporative enrichment and potentially by mixing with ground water.

106   Plants take up water which carries this precipitation or soil water $\delta^{18}O$ signature. During transport
107   from roots to leaves isotope ratios are not modified (Wershaw et al., 1966). In the leaves, water
108   becomes enriched in ^{18}O relative to source water as a result of transpiration (Dongmann et al.,
109   1974). The enrichment at the site of evaporation (the stomata) is primarily driven by the ratio of
110   the vapor pressure outside versus inside the leaf. Source water (i.e. soil water) that enters the leaf
111   via the transpirational stream, mixes with the ^{18}O-enriched water and dilutes the leaf water $\delta^{18}O$
112   signal (a Péclet effect, Barbour et al., 2004). This Péclet effect tends to reduce the signal of
113   evaporative enrichment in bulk leaf water (i.e. whole leaf water) and the effect is large when
114   transpiration rates are high. Sucrose formed in the leaves is thought to be 27‰ enriched in ^{18}O
115   compared to leaf water due to fractionation during the exchange of oxygen between carbonyl
116   groups in organic molecule and water (Sternberg et al., 1986). Sugars are then transported down
117   the trunk where partial exchange with xylem water occurs before tree-ring cellulose is formed
118   (Roden et al., 2000; Gessler et al., 2014). Based on isotope theory, oxygen isotope ratios in tree
119   rings serve as proxy data for relative humidity and reflect the signature of soil water (McCarroll
120   and Loader, 2004). The relative strength of the humidity and soil water signal, however, is
121   expected to vary due to the Péclet effect and oxygen isotope exchange during stem cellulose
122   formation (see below) and is often difficult to quantify, which somewhat hampers current
123   interpretation of tree-ring results.

124   Tree ring chronologies have been found to correlate with relative humidity (Burk and Stuiver,
125   1981; An et al., 2014; Xu et al., 2014) and $\delta^{18}O$ of precipitation (Waterhouse et al., 2002). In
126   addition, tree ring $\delta^{18}O$ archives are proxies for e.g. precipitation amounts (Treydte et al., 2006),

---

Sonja Keel 3/2/2016 8:28 PM
Deleted: (Fig. 1)

Sonja Keel 3/29/2016 9:51 AM
Deleted: Unless oxygen isotope ratios are modified through evaporation or mixing with ground water,

Weigt Rosemarie B…, 3/29/2016 3:01 PM
Formatted: English (US)

Weigt Rosemarie B…, 3/29/2016 3:01 PM
Formatted: English (US)

Weigt Rosemarie B…, 3/29/2016 3:01 PM
Formatted: English (US)

Sonja Keel 3/2/2016 8:30 PM
Deleted: the $\delta^{18}O$ of surface soil water corresponds to that of precipitation averaged over a certain amount of time

Weigt Rosemarie B…, 3/29/2016 3:01 PM
Formatted: English (US)

Sonja Keel 3/2/2016 8:31 PM
Deleted: Bulk leaf water is therefore less ^{18}O-enriched when transpiration rates are high.

4

136   the occurrence of droughts (Masson-Delmotte et al., 2005; Herweijer et al., 2007) and tropical

137   cyclones (Miller et al., 2006), or leaf-to-air vapor pressure differences (Kahmen et al., 2011).

138   Regarding tree rings, $\delta^{18}O$ in stem cellulose has been described with mechanistic models to

139   characterize the transfer of $\delta^{18}O$ signals from soil water to stem cellulose (Roden et al., 2000;

140   Cernusak et al., 2005; Barbour, 2007; Gessler et al., 2009, Ogée et al. 2009). A formulation of

141   leaf water enrichment at the site of evaporation (i.e. the stomata) based on the model by Craig and

142   Gordon (1965) is common to all models, but additional processes related to $\delta^{18}O$ signals in leaf

143   water and stem cellulose are resolved at varying degrees of complexity. Some models include

144   boundary layer considerations (Flanagan et al., 1991) or the Péclet effects that reduce leaf water

145   enrichment (Barbour et al., 2004; Farquhar and Gan, 2003). Others account for variations in

146   isotopic exchange of oxygen with xylem water (Barbour and Farquhar, 2000), or weight diurnal

147   variations in leaf water enrichment by photosynthetic rates (Cernusak et al., 2005). Here, we use a

148   rather general approach with a single Péclet effect and constant isotopic exchange with xylem

149   water, as we aim to simulate stem cellulose across a large range of different species, and as we

150   lack detailed species-specific information, e.g. on water flow and the Péclet effect. On the other

151   hand, we move a step forward in that we integrate a mechanistic model for stem cellulose $\delta^{18}O$

152   into a DGVM that allows us to cover large spatial and temporal scales and that explicitly

153   considers numerous hydrological and physiological processes.

154

155   **2   Material and methods**

156   **2.1   Model description**

157   Stable oxygen isotopes were implemented in the LPX-Bern DGVM (Land surface Processes and

158   eXchanges, Bern version 1.0) (Spahni et al., 2013; Stocker et al., 2013). LPX-Bern describes the

159   evolution of vegetation cover, carbon (C) and nitrogen (N) dynamics in soil and vegetation, and

160   the exchange of water, CO_2, C isotopes, methane, and nitrous oxide between the atmosphere and

161   the land biosphere.

162   The model version applied here features a horizontal resolution of 3.75 x 2.5 degree, a vertically

163   resolved soil hydrology with heat diffusion and an interactive thawing-freezing scheme (Gerten et

al., 2004; Wania et al., 2009), and features a daily time step for photosynthesis and evapotranspiration. The soil hydrology scheme is similar to a concurrent LPX version (Murray et al., 2011; Prentice et al., 2011). There are ten plant functional types (PFTs) that have distinct bioclimatic limits and differ in their physiological traits such as minimum canopy conductance (Sitch et al., 2003) (Table S2 in Ruosch et al., 2016). The distribution of fine roots in the soil profile is also PFT-specific and leads to competition for water. Light competition is modeled indirectly by assigning a higher mortality to PFTs with a small increment in fractional plant cover and biomass compared to PFTs with a large increment (Sitch et al., 2003). Daily evapotranspiration is calculated for each PFT as the minimum of a plant- and soil-limited supply function (E_{supply}) and the demand for transpiration (E_{demand}). E_{supply} is the product of root-weighted soil moisture availability and a maximum water supply rate that is equal for all PFTs (Sitch et al., 2003). E_{demand} is calculated following Monteith's (Monteith, 1995) empirical relation between evaporation efficiency and surface conductance,

$$E_{demand} = E_{eq}\,\alpha_m\left[1 - \exp\left(\frac{-g_c\,\phi}{g_m}\right)\right], \tag{1}$$

where E_{eq} is the equilibrium evaporation rate, g_m and α_m are empirical parameters that are equal for all plant functional types, g_c the canopy conductance, and ϕ the fraction of present foliage area to ground area (i.e. projected leaf area). Equation (1) is solved for E_{demand} using the non-water-stressed potential canopy conductance as calculated by the photosynthesis routine for a fixed ratio λ between the CO_2 mole fraction in the stomatal cavity and the ambient air. λ is set equal to 0.8 following Sitch et al. (2003) to approximate non-water-stressed conditions and as a starting value for the iterative computation of carbon assimilation and transpiration. In case of water-stressed conditions when E_{demand} exceeds E_{supply}, canopy conductance and photosynthesis are jointly and consistently down-regulated; E_{demand} is set to E_{supply} and Equation 1 is solved for g_c.

Photosynthesis is modeled following Collatz et al. (1991; 1992), which is based on the formulations by Farquhar et al. (1980) and Farquhar and von Caemmerer (1982) generalized for global modeling purposes. The N content and Rubisco activity of leaves are assumed to vary seasonally and with canopy position in a way to maximize net assimilation at the leaf level. For C_3 plants assimilation is a function of the daily integral of absorbed photosynthetically active

209   radiation. For a detailed description see Haxeltine and Prentice (1996b, a).

210   Canopy conductance, g_c, is linked to daytime assimilation, A_{dt}, through

$$g_c = g_{min} + \frac{1.6 A_{dt}}{[c_a(1-\lambda)]},\qquad(2)$$

211   where g_{min} is a PFT specific minimum canopy conductance and c_a is the ambient mole fraction of
212   CO_2 and λ the ratio between the CO_2 mole fraction in the stomatal cavity and the ambient air. The
213   equations for water supply and demand, assimilation, and canopy conductance are solved
214   simultaneously by varying λ to yield self-consistent values for λ, g_c, assimilation and
215   transpiration.

216   2.2   Leaf water and stem cellulose $\delta^{18}O$ model

217   To calculate $\delta^{18}O$ in leaf water we use the Péclet modified Craig-Gordon (PMCG) model as
218   described e.g. in Farquhar & Lloyd (1993).

219   The evaporative enrichment of leaf water above the plant's source water at the site of evaporation
220   ($\Delta^{18}O_e$), is based on the Craig-Gordon formulation (Craig and Gordon, 1965; Dongmann et al.,
221   1974)

$$\Delta^{18}O_e = \varepsilon^+ + \varepsilon_k + (\Delta^{18}O_v - \varepsilon_k)\frac{e_a}{e_i},\qquad(3)$$

223   where ε^+ is the temperature-dependent equilibrium fractionation factor between liquid and vapor
224   water and is calculated as

$$\varepsilon^+ = 2.644 - 3.206(\frac{10^3}{T_l}) + 1.534(\frac{10^6}{T_l^2}) \; (‰),\qquad(4)$$

226   with T_l the leaf temperature in K (Bottinga and Craig, 1969 in Barbour, 2007). ε^+ increases with
227   decreasing temperature and is around 8.8‰ at 30 C and around 11.5‰ at 0 C. ε_k is the kinetic
228   fractionation factor for water vapor diffusion from the leaf to the atmosphere (32‰; Cappa et al.,
229   2003), $\Delta^{18}O_V$ describes the oxygen isotope enrichment of water vapor in the atmosphere above
230   source water, and e_a/e_i is the ratio of ambient to intercellular vapor pressures. This ratio is equal
231   to relative humidity when leaf and air temperatures are similar and e_i is at saturation pressure. We

235 assume that leaf temperature is approximated by air temperature (see also Discussion). We use

236 this formulation in LPX-Bern for the comparison against published leaf water $\delta^{18}O$ (West et al.,

237 2008).

238 All other results were derived with the expanded model that includes a Péclet effect. The Péclet

239 number is defined as

240 $$\wp = \frac{LE}{cD},\tag{5}$$

241 and accounts for the dilution of ^{18}O-enriched leaf water by unenriched source water that enters

242 the leaf via the transpirational stream (E, mol m^{-2} s^{-1}) and is effective over a path length L

243 (Farquhar and Lloyd, 1993). To keep the model as simple as possible we set L to 0.03 m for all

244 PFTs following Kahmen et al. (2011), although L can vary largely between species (Kahmen et

245 al., 2009), c is the molar density of water (55.5 × 10^3 mol m^{-3}) and D the temperature dependent

246 diffusivity of H$_2$^{18}O in water (Cuntz et al., 2007, Equation A22, Typo corrected: 10^{-8} instead of

247 10^{-9}):

248 $$D = 10^{-8} \exp(-0.4 + \frac{1528}{T_l} + \frac{-554368}{T_l^2}) \ (\text{m}^2 \ \text{s}^{-1})\tag{6}.$$

249 Bulk leaf water ^{18}O enrichment can then be calculated as

250 $$\Delta^{18}O_{LW} = \frac{\Delta^{18}O_e(1 - e^{-\wp})}{\wp}\tag{7}$$

251 $\Delta^{18}O_{LW}$ is smaller than $\Delta^{18}O_e$ and approaches $\Delta^{18}O_e$ for small transpiration rates E. In regions with

252 high leaf transpiration rates such as high latitudes the reduction of $\Delta^{18}O_e$ due to the Péclet effect is

253 most strongly expressed (Fig. S1 in the Supplement). Leaf water $\delta^{18}O$ is

254 $$\delta^{18}O_{LW} = \Delta^{18}O_{LW} + \delta^{18}O_{SW}\tag{8}$$

255 where $\delta^{18}O_{SW}$ refers to soil water $\delta^{18}O$. Stem cellulose isotopic composition is calculated as

256 $$\delta^{18}O_{SC} = p_{ex}p_x(\delta^{18}O_{SW} + \varepsilon_{wc}) + (1 - p_{ex}p_x)(\delta^{18}O_{LW} + \varepsilon_{wc})$$

257 $$= \delta^{18}O_{SW} + (1 - p_{ex}p_x)\Delta^{18}O_{LW} + \varepsilon_{wc},\tag{9}$$

258 where ε_{wc} is the fractionation between $\delta^{18}O$ of water and the $\delta^{18}O$ of the primary products of

262 photosynthesis of 27‰ (Epstein et al., 1977), p_{ex} is the proportion of exchangeable oxygen in

263 cellulose formed from sucrose, and p_x is the proportion of $\delta^{18}O_{SW}$ at the site of cellulose

264 formation (Roden et al., 2000). For our simulations we used values of 0.4 for p_{ex} (Cernusak et al.,

265 2005; Sternberg, 2009) and 1.0 for p_x (Kahmen et al., 2011).

266 Photosynthesis and plant water fluxes and thus changes in leaf water and stem cellulose $\delta^{18}O$ are

267 computed with a daily time step. Because stem cellulose formation is restricted to the vegetation

268 period in temperate and boreal regions, we apply positive net primary production (NPP) as weight

269 to compute time-averaged stem cellulose and leaf water $\delta^{18}O$ and apply a cutoff of 1.0 g C m^{-2}

270 month^{-1}. This means that annual $\delta^{18}O$ of stem cellulose is calculated only based on months with a

271 NPP higher than 1.0 g C m^{-2} month^{-1} and months with high NPP have a stronger weight. Effects

272 of C storage related to the incorporation of photoassimilates from previous years into current

273 year's cellulose is not accounted for (Gessler et al., 2007).

2.3 Input data

275 Monthly gridded meteorological data (temperature, precipitation, cloud cover, and number of wet

276 days (CRU TS v. 3.21; Harris et al., 2014), annual atmospheric N-deposition fields (Lamarque et

277 al., 2011), and atmospheric CO_2 (Etheridge et al., 1998; MacFarling Meure et al., 2006) are

278 prescribed to LPX-Bern. The meteorological data are linearly interpolated to daily values, except

279 for precipitation where a stochastic weather generator is applied to compute daily precipitation

280 following Gerten et al. (2004). Monthly soil water $\delta^{18}O$, water vapor $\delta^{18}O$ and relative humidity

281 data are from a simulation with the coupled atmosphere-land surface model ECHAM5-JSBACH

282 for the period 1960 to 2012 (Haese et al., 2013) .

283 Next, the CRU climate input data are briefly evaluated. For five tree-ring sites in Switzerland (see

284 section 2.5), we compared the CRU climate input data against relative humidity from

285 meteorological stations (Source MeteoSwiss) and homogenized air temperature and precipitation

286 data for Switzerland (Begert et al., 2005). For the high-elevation site at Davos (DAV)

287 summertime (June-August, JJA) precipitation and relative humidity input data are slightly higher

288 than data from meteorological stations in the 1960s and 70s and similar thereafter. Air

289 temperatures for the corresponding pixel from the gridded CRU data set are around 4 °C higher

290 than in the MeteoSwiss data at DAV, as the CRU data represent averages for a large area. The

298 CRU data for the sites LOV and LOT compare relatively well with the meteorological station
299 data, except for higher precipitation (both sites) and higher air temperature (site LOT).

300 A first-order correction is applied to the relative humidity data from ECHAM5-JSBACH to
301 account for the daily cycle. Leaf water ^{18}O enrichment is driven by daytime relative humidity
302 (when stomata are open), whereas the available ECHAM5-JSBACH data represent 24-hour
303 averages. Relative humidity is reduced uniformly by an absolute value of 10% based on a
304 comparison of 24-hour against 8:00-18:00 summertime average relative humidity values in
305 temperate and boreal regions (Kearney et al., 2014). This correction was evaluated for a few
306 summer days at the site DAV and found to be sufficient.

307 ECHAM5-JSBACH includes the atmosphere model ECHAM5 (Roeckner et al., 2003), and the
308 land surface scheme JSBACH (Jena Scheme for Biosphere-Atmosphere Interaction in Hamburg;
309 Raddatz et al., 2007). The model comprises three surface water reservoirs: a snow layer, water at
310 the skin layer of the canopy or bare soil, and a soil water layer. These three pools are each
311 represented by a single layer bucket model, and each of them has a prescribed maximum field
312 capacity. In ECHAM5-JSBACH, there are no soil layers and the isotopic composition has no
313 vertical gradient. Any water taken up by plants has the δ^{18}O of soil water. The soil layers in LPX-
314 Bern do not affect the isotopic composition, but are exclusively used for quantitative assessment
315 of water pools and fluxes. The drainage to groundwater in ECHAM5-JSBACH has the isotopic
316 composition of the soil water. No fractionation during snowmelt is assumed. Liquid precipitation
317 and melt water are added to the skin layer reservoir and the soil reservoir, respectively. After
318 these reservoirs are filled, the residual water yields the runoff.

319 In order to calculate evapotranspiration in ECHAM5-JSBACH, each grid cell is divided into four
320 cover fractions: one covered by snow, one covered with water in the skin layer reservoir, one
321 covered by vegetation, and one covered by bare soil. The complete evapotranspiration flux is
322 calculated by the weighted sum of these four fractions. The skin layer is modeled as a thin layer
323 of water, which in general evaporates completely within a few model time steps.

2.4 Simulations

A spinup of 1500 years is performed with LPX-Bern, where an analytical solution for the C inventory in slow soil pools is applied after 1000 years to ensure that all C pools have established equilibrium conditions by the end of the spinup. Atmospheric CO_2 concentrations of the year 1900, atmospheric N deposition rates of 1901, climate data from 1901-1931, and $\delta^{18}O$ input data for 1960 are used during the spinup. Transient simulations are started in 1901 forced by atmospheric CO_2, annual N deposition (Lamarque et al., 2011), and monthly climate (see section 2.3). For the years 1901-1960 we use monthly relative humidity, soil water $\delta^{18}O$ and vapor $\delta^{18}O$ of 1960 and 1960-2012 data thereafter. All runs are for potential vegetation (no land use) and feedbacks between C and N cycles are enabled (i.e. potential limitation of growth by low N availability).

In factorial simulations, model parameters or input data are increased individually by 10% and the impact is evaluated for stem cellulose $\delta^{18}O$ for the June, July, and August 1960 average for the grid cell that includes the site DAV. In another suite of sensitivity experiments the influence of 20th century trends and variability on simulated $\delta^{18}O$ is explored (see section 3.3). Individual input data are kept at initial conditions, while all others are prescribed as in the standard simulation. For these sensitivity experiments monthly means of 1901-1931 are applied for air temperature, precipitation, cloud cover, and number of wet days), and monthly means of 1960-1969 for relative humidity, soil water $\delta^{18}O$ and water vapor $\delta^{18}O$, and 1901 values for atmospheric CO_2 and N deposition. In a similar factorial experiment, the Péclet effect is excluded. The time series are smoothed using Stineman functions. For the site DAV we carry out an additional series of experiments to evaluate the influence of a 3.5°C lower leaf than air temperature (because the 1960-2012 mean measured temperature is 3.5°C lower than the CRU temperature used in LPX-Bern), a temperature dependent biochemical fractionation as described in Sternberg and Ellsworth (2011),

$$\varepsilon_{wc} = 0.0084T^2 - 0.51T + 33.172 \; , \tag{10}$$

and this temperature dependent biochemical fractionation with measured air temperature prescribed instead of the default CRU data, while all other terms remain unchanged.

11

2.5 Tree-ring δ^{18}O data

To validate our model with regard to spatial variations, we compare mean δ^{18}O of stem cellulose for the years 1960-1996 (or until 2012 depending on availability of data) against observations from 31 sites in temperate and boreal forests (Treydte et al., 2006, 2007, 2009; Kress et al., 2010; Holzkämper et al., 2011). The sites span an area from Spain to Pakistan in the east-west and in the North-South from Morocco to Finland, but the majority is located in Europe. Measurements were performed on different tree species. In most cases, the corresponding plant functional type (temperate broad-leaved summergreen, temperate or boreal needle-leaved evergreen, or boreal needle-leaved summergreen) is simulated by LPX-Bern at the location of interest and used for model-data comparison. Otherwise, we use simulated δ^{18}O values of the dominant tree plant functional type simulated by the model. This is permissible as the differences in δ^{18}O between functional types are rather minor (see below).

Five sites in Switzerland were chosen for a comparison of time series (Table S1). DAV is a West-facing site at 1660 m above sea level (asl) dominated by the evergreen *Picea abies* (L.) H. Karst near the village of Davos. The sites on the mountain Lägern (LAEA and LAEB), situated on similar altitudes of about 720 m asl, have a South aspect, but are on different soil types. Site LAEA is on sandstone and is dominated by the deciduous broad-leaved *Fagus sylvatica* L. and the evergreen needle-leaved *Abies alba* Mill., the site LAEB is on limestone and is dominated by the two deciduous broad-leaved species *F. sylvatica* and *Fraxinus excelsior* L. However, only *F. sylvatica* is analysed here. The North-facing site in the Lötschen Valley (N19) is at 2000 m asl and is dominated by the evergreen *P. abies*. Close by is an additional site LOE in the Lötschen Valley at 2100 m asl that has a South-North exposure and is dominated by *L. decidua* (Kress et al., 2010).

For two additional sites in the Lötschen Valley at 1350 m asl and 2100 m asl (LOV, LOT), a complete set of input data at about bi-weekly resolution for the year 2008 including soil and needle water δ^{18}O for *Larix decidua* L. was available (Treydte et al., 2014). The site LOT is in immediate neighborhood to the site LOE but different trees were sampled at the two sites. In contrast to all other sites, whole wood δ^{18}O was analyzed instead of cellulose. We therefore

increased the whole wood values by 4.0 ‰ to convert them to cellulose, according to the constant difference documented in larch for the last decades (Sidorova et al., 2008).

While most of these measured tree-ring $\delta^{18}O$ chronologies were derived from pooled samplings of 4-5 dominant trees (Treydte et al. 2007, Kress et al. 2010), the dataset of the sites DAV, LAEA, LAEB and N19 was based on measurements of individual trees, sampled within the framework of the present study. Here, the sampling design covered not only dominant but also smaller trees within a circular plot of about 30 m in diameter, in order to account for the full range of tree ring isotopic signature within a stand (Babst et al., 2014). From about 10 trees per site stable oxygen isotope ratios were measured separately for each selected tree and each year over the full length of the sampled cores. Tree ring cellulose was extracted prior to measurement of $\delta^{18}O$ via pyrolysis (PYRO-cube, Elementar, Hanau, Germany) and analysed for $\delta^{18}O$ by isotope ratio mass spectrometry (Delta Plus XP IRMS, ThermoFinnigan MAT, Bremen, Germany), as described in Weigt et al. (2015). Mean values of the individual trees per year were used for site-specific $\delta^{18}O$ chronologies.

3   Results

3.1   Large scale, global patterns of $\delta^{18}O$ in soil water, leaf water, and stem cellulose

We first analyze the large scale, global patterns of $\delta^{18}O$ in soil and leaf water and in stem cellulose to identify characteristic features and to evaluate the plausibility of simulated results. Annual mean soil water $\delta^{18}O$ values simulated by ECHAM5-JSBACH range between -1 and -21 ‰ (1960-1990; Fig. 1) and are in the same range as reconstructions of $\delta^{18}O$ in precipitation from the Global Network for Isotopes in Precipitation (GNIP) database (Bowen and Revenaugh, 2003). For precipitation, Haease et al. (2013) estimates that the root mean square error between precipitation $\delta^{18}O$ simulated by ECHAM5-JSBACH and the GNIP data is 1.78 ‰. The simulated soil water $\delta^{18}O$ pattern represents major features as identified for $\delta^{18}O$ in precipitation (e.g., Bowen and Revenaugh, 2003). Namely, a decrease in $\delta^{18}O$ from mid-latitudes to high latitudes, lower signatures at high elevation, and a decrease from coastal regions towards the continental

13

Sonja Keel 4/1/2016 9:35 AM
Deleted: Tree cores from 10 trees per site were sampled and cut by each year. The tree

Weigt Rosemarie B…, 3/29/2016 4:55 PM
Deleted: 9

Weigt Rosemarie B…, 3/29/2016 4:55 PM
Deleted: 6

443 interior. The simulated soil water δ^{18}O pattern generally agrees with the pattern interpolated for

444 precipitation from the GNIP data (Bowen and Revenaugh, 2003).

445 Simulated leaf water δ^{18}O averaged across all plant functional types range from about -14‰ at

446 high latitudes to about 28‰ in the Middle East (Fig. 2, upper panel). Thus, the simulated δ^{18}O

447 values in leaf water at the grid-cell and climatological scale span a range of ~40‰. δ^{18}O values in

448 leaf water result from the combination of soil water δ^{18}O and evaporative enrichment. There are

449 also substantial regional differences in the evaporative enrichment of δ^{18}O in leaf water mainly

450 due to large differences in air humidity, i.e. higher enrichment in arid regions than high latitude

451 regions (Fig. 3a). These differences are much larger than the differences between annual mean

452 δ^{18}O in soil water from ECHAM5-JSBACH and reconstructed δ^{18}O in precipitation discussed in

453 the previous paragraph. This suggests that soil water δ^{18}O fields from ECHAM5 provide a

454 reasonable input to force LPX-Bern simulations and that evaporative enrichment is a major

455 process shaping the spatial pattern in leaf water δ^{18}O.

456 West et al. (2008) combined annual average δ^{18}O data in precipitation (Bowen and Revenaugh,

457 2003), monthly climatology for air temperature and relative humidity, and elevation data with the

458 Craig-Gordon formulation for evaporative enrichment to estimate leaf water δ^{18}O. Our values

459 roughly agree with the Geographic Information System (GIS) model by West et al. (2008)(Fig. 2,

460 lower panel), but differences exist in many regions. Our estimates tend to be substantially higher

461 in e.g. Western Amazonia, Central Siberia and the Middle East, while they are significantly lower

462 for small regions in Central Africa and China. Leaf water δ^{18}O in Australia and Eastern Russia

463 agree comparatively well.

464 Differences in simulated leaf water δ^{18}O between the two approaches are much larger than

465 differences between annual mean δ^{18}O in precipitation, used by West et al. (2008) as input to

466 their GIS approach, and annual mean δ^{18}O in soil water from ECHAM5-JSBACH. Thus,

467 uncertainties in the source water input data do not explain the differences between the two

468 approaches. The mechanistic approach implemented in LPX-Bern to model leaf water isotopic

469 signatures considers seasonally varying δ^{18}O of both, source water and atmospheric water vapor,

470 and models explicitly daily stomatal conductance, transpiration, and associated δ^{18}O transport.

Sonja Keel 4/1/2016 9:37 AM
Deleted: s

Sonja Keel 3/2/2016 8:56 PM
Deleted: 5

Tree ring cellulose δ^{18}O is in the expected range for most regions (Fig. 3b). Generally values are higher in arid regions and lower at high latitudes and range between 15 and 35‰ (Saurer et al., 2002; Ferrio and Voltas, 2005). When comparing leaf water and stem cellulose δ^{18}O with the δ^{18}O forcing used (Figs. 1, 2, 3b), it is obvious that soil water, leaf water, and cellulose δ^{18}O share a common pattern as described above. However, the simulated range of δ^{18}O in cellulose is comparable to the δ^{18}O range in soil water (or precipitation), but only half as large as the δ^{18}O range in leaf water. Due to biochemical fractionation during cellulose synthesis (ε_{wc}), cellulose δ^{18}O is up to 27 ‰ higher compared to leaf water δ^{18}O and cellulose depends linearly on leaf water δ^{18}O. The difference between stem cellulose and leaf water δ^{18}O can be calculated by combining equations 8 and 9 and this yields a simple linear relationship with leaf water enrichment ($\delta^{18}O_{SC}$ - $\delta^{18}O_{LW}$ = ε_{wc} - $p_{ex}p_x$ $\Delta^{18}O_{LW}$, where $p_{ex}p_x$ is 0.4 and ε_{wc}=27‰). The difference between cellulose and leaf water δ^{18}O is thus highest in regions with very low leaf water enrichment such as at high latitudes. The simulated enrichment of stem cellulose with respect to soil water is also proportional to leaf water enrichment ($\delta^{18}O_{SC}$ - $\delta^{18}O_{SW}$ = $\Delta^{18}O_{LW}$ (1-$p_{ex}p_x$) + ε_{wc}). The slope of this relationship is with 0.6 (1 - $p_{ex}p_x$, $p_{ex}p_x$ = 0.4) smaller than unity, which explains the smaller spatial gradients in stem cellulose δ^{18}O compared to leaf water δ^{18}O.

3.2 Comparison of simulated stem cellulose δ^{18}O with tree ring data

Next, we quantitatively evaluate simulated δ^{18}O in stem cellulose by comparing modeled long-term (~50-yr) averages at individual grid cells with measured δ^{18}O from local, site-specific tree ring data (Table S1 in the Supplement). We recall that LPX-Bern is run with a resolution of 3.75° x 2.5° which implies mismatches between local site conditions (altitude, climate, etc.) and grid-cell averages as used to force the model. Nevertheless, simulated stem cellulose δ^{18}O agrees well with measured tree ring data from 31 sites mainly located in European temperate and boreal forests (circles in Fig. 3b, Fig. 4). The model captures the observation-based range in δ^{18}O for these sites from about 26 to 32‰ and the correlation between model and tree ring data is $r = 0.71$ across all data points. In general the model tends to underestimate δ^{18}O values of stem cellulose. Modeled grid cell values at five Swiss sites, that will be used to explore temporal dynamics, also show somewhat lower δ^{18}O in stem cellulose (0-2‰) than the tree ring δ^{18}O data suggest (Fig. 5).

15

512 This holds for the alpine, high altitude sites at DAV (Fig. 5a) and in the Lötschen Valley (N19,

513 LOE, Fig. 5j,k) as well as for the low-lying sites in the Swiss Central Plateau (LAEA, LAEB,

514 Fig. 5h,i). The low bias is most strongly expressed at sites where the model is forced by very high

515 relative humidity (annual mean 1960-2012 weighted by NPP is >80%, Fig. 4 green symbols (sites

516 FON, GUT, INA, LIL, MOT)). This bias at high humidity sites could potentially arise from a bias

517 in $\delta^{18}O$ of soil water, in $\delta^{18}O$ of water vapor, or in relative humidity, and thus vapor pressure

518 deficit, and could be related to differences in the spatial scale, i.e. local measurements at

519 individual trees versus averages over all trees of a plant functional type and over a grid cell. We

520 note that daily-average relative humidity is reduced by 10% for the simulation of leaf water $\delta^{18}O$

521 to account for the lower daytime vs. 24-hour humidity; uncertainties in this correction have a

522 larger influence on the water vapor pressure deficit, the driving force for transpiration, at humid

523 sites. At a single site (CAZ) where LPX-Bern simulates extremely low biomass of less than 30 g

524 C m^{-2}, because herbaceous plants dominate in this grid cell, stem cellulose $\delta^{18}O$ is also

525 underestimated (open symbol in Fig. 4). Excluding this site and the very humid sites yields a

526 correlation coefficient of $r = 0.65$, which is not higher than for all sites. We conclude that LPX-

527 Bern is able to represent the magnitude and the spatial climatological pattern of $\delta^{18}O$ in stem

528 cellulose in Europe, generally within a few per mil of available observations.

529

530 This conclusion is further corroborated by comparing LPX-Bern results with $\delta^{18}O$ data from two

531 Swiss sites (LOV, LOT) for which detailed $\delta^{18}O$ data are available for soil water, needle water,

532 and stem wood (Table 1), but for a single year only. Simulated enrichment of needle water above

533 soil water as well as simulated enrichment of stem cellulose above needle water is within the

534 observed range at the two sites (Table 1). We note that this comparison is somewhat hampered by

535 the large variability in the weekly samples (e.g., for leaf water $\delta^{18}O$ at LOV: 3.9-16.4‰ and at

536 LOT: -4.6-11.4‰) that LPX-Bern cannot reproduce because the model is driven by monthly data.

537 The inter-annual variability and decadal-scale trends of stem cellulose $\delta^{18}O$ are analyzed for five

538 tree ring sites in Switzerland and for the period 1960 to 2012 for which temporally resolved input

539 data from ECHAM5-JSBACH are available (Fig. 5). Due to the coarse spatial resolution of the

540 gridded LPX-Bern version applied here, all sites except DAV lie within the same grid cell and

541 model results are almost identical. Slight differences in the model time series shown in Figure 5,

are due to differences in tree functional types (LAEA/LAEB: deciduous broad-leaved, N19: evergreen needle-leaved, LOE: deciduous needle-leaved; thin lines in Fig. 5h-k) selected for the comparison with the tree ring $\delta^{18}O$ data.

The simulated stem cellulose $\delta^{18}O$ time series capture the measured evolution and inter-annual variability (Fig. 5a,h-k). Based on visual comparison, the correlation between simulated and measured stem cellulose $\delta^{18}O$ is best in the 60s and early 70s and is weaker thereafter. Model values increase after 1990 probably due to higher temperature and soil water $\delta^{18}O$, which is not recognized in the tree ring data. For the entire time series the correlations range between 0.48 and 0.73, with the highest value at LAEA in the Swiss central plateau (Fig. 5h) and the lowest value at the alpine site DAV (Fig. 5a). The correlation coefficients are comparable to the correlations between the four tree ring series in the Swiss Central Plateau (LAEA, LAEB) and the Lötschen Valley (N19, LOE) which range between 0.55 and 0.82. In other words, the correlation between measured and modeled grid cell values reflects site-to-site variability within the grid-cell. In conclusion, not only the reconstructed climatological mean pattern across Europe, but also the reconstructed temporal variability in stem cellulose $\delta^{18}O$ at individual Swiss sites is generally well represented by LPX-Bern.

An extreme heat wave hit Europe in 2003 (Figs. 5, 7, S2, and S3) with summer temperatures of 3°C above the 1961 to 1990 mean (Schär et al., 2004) and one expects to find extreme values in $\delta^{18}O$. Indeed, simulated stem cellulose $\delta^{18}O$ peaks in this year with record or near-record high values for the analysis period (Fig. 5). Very low humidity and high air temperatures most likely lead to strong leaf water $\delta^{18}O$ enrichment. Surprisingly, the response in $\delta^{18}O$ in the tree ring data is different for different sites. Measurements at LAEA, N19, and LOE show a strong peak in $\delta^{18}O$ (Fig. 5h,j,k), DAV a small peak (Fig. 5a), and site LAEB even lower values than during the previous and following year (Fig. 5i). Apparently, local differences in conditions or different reactions of different tree species may mask the expected drought signal in stem cellulose $\delta^{18}O$. A well-known phenomenon is that extreme conditions may not be captured because growth is stopped and the signal therefore not recorded (Sarris et al. 2013).

17

3.3 Sensitivity analysis to explore the influence of individual drivers

Simulated variability in stem cellulose $\delta^{18}O$ arises from various drivers and their influence is quantified within LPX-Bern. In the standard simulation with the combination of all drivers, air temperature, soil water $\delta^{18}O$ and water vapor $\delta^{18}O$ are positively correlated with cellulose $\delta^{18}O$ as demonstrated for site DAV (Fig. 5b,d,e). In contrast, relative humidity and precipitation are negatively correlated with cellulose $\delta^{18}O$ (Fig. 5c,f). The correlation is strongest with soil water $\delta^{18}O$ suggesting a high dependence of our results on the isotope input data.

The influence of various drivers on cellulose $\delta^{18}O$ is further investigated in transient factorial simulations where individual drivers were kept at their climatological mean values representative for the early 20th century for the meteorological variables temperature, precipitation, cloud cover, and number of wet days, and 1960 values for relative humidity, $\delta^{18}O$ soil water and water vapor input data. The results (Fig. 6) show that, in order of importance, variations in relative humidity, temperature, $\delta^{18}O$ in soil water, and water vapor $\delta^{18}O$ force decadal-scale and inter-annual variability in cellulose $\delta^{18}O$. The simple sensitivity analysis for the site DAV, where input data or parameters were increased by 10%, also reveals that stem cellulose $\delta^{18}O$ is sensitive to changes in relative humidity, soil water and water vapor $\delta^{18}O$ (Table 2). Precipitation had no influence on stem cellulose $\delta^{18}O$ in the transient simulation (Fig. 6a). In contrast, accounting for the Péclet effect, resulted in consistently lower values with nearly no influence on inter-annual variation (Fig. 6b). Atmospheric CO_2 had a very minor effect on cellulose $\delta^{18}O$ (<0.04‰ except for a single year with an effect of 0.18‰), while N deposition had no influence (Fig. 6b). In years when relative humidity and temperature had a positive effect, the combined effect of temperature, precipitation, number of wet days and cloud cover (termed "clim effect" in Fig. 6a) was often large and also positive. In years when the influence of relative humidity and temperature had opposing signs, the clim effect was around zero. The 20th century trends in air temperature mostly led to higher stem cellulose $\delta^{18}O$ during the last five decades compared to the early 20th century. The clim effect leads to slightly higher decadal-averaged values in stem cellulose $\delta^{18}O$ (+0-2‰) towards the end of the simulation. However, these values are not unusual in the context of the decadal variability simulated for the past five decades.

Sensitivities of cellulose $\delta^{18}O$ to the input data are similar at all sites (Fig. 6c-e). Compared to DAV, the magnitude of the decadal-scale trends induced by "climate" and soil water $\delta^{18}O$ changes are somewhat smaller at other sites though. Conversely, changes in relative humidity have a stronger influence at LAEB and N19. At all sites, the prescribed changes in relative humidity (i.e. keeping values at mean representative for the early 20th century) cause on average lower cellulose $\delta^{18}O$ during the 1980s than compared to the end of the simulation. Decadal-scale variability is also related to changes in soil water $\delta^{18}O$. In particular, soil water $\delta^{18}O$ variations caused an increase in stem cellulose $\delta^{18}O$ of about 0.3 to 0.5 ‰ in the 1980s that persisted thereafter (Fig. 6e). A similar trend was simulated for "climate", but with more variability between sites. At N19 the "climate" effect was always lowest and there was no clear trend. In brief, LPX-Bern simulates substantial inter-annual and decadal scale variability in stem cellulose $\delta^{18}O$ which is attributable to variability in relative humidity, temperature, and $\delta^{18}O$ in soil water and vapor.

West et al. (2008) assumed that leaf temperature exceeds air temperature by 5°C in their implementation of the Craig-Gordon model. Since CRU air temperatures are on average 3.5°C higher than measured temperatures for the Swiss site DAV (Fig. 7), we did not want to further increase them. Instead we tested the effect of reducing leaf temperature by 3.5°C compared to air temperature, which improved the correlation of simulated and measured stem cellulose $\delta^{18}O$ at DAV and increased the simulated stem cellulose $\delta^{18}O$ compared to the original simulation (Fig. 8, 'Tleaf' vs. 'LPX-Bern standard simulation': 27.05‰ vs. 26.47‰ (average for 1960-2012)). Similarly, accounting for a temperature dependent biochemical fractionation ('ewcT') led to consistently higher cellulose $\delta^{18}O$ (27.21‰) compared to the standard simulation, with a nearly identical correlation coefficient compared to the 'Tleaf' simulation. When the temperature-dependent formulation for ε_{wc} was combined with temperature forcing from a nearby meteorological station ('ewcTmeteo'), stem cellulose $\delta^{18}O$ increased further and was even slightly higher than the measured data (28.47‰ vs. 28.02‰, average for 1960-2012). The correlation remained equally good though compared to the simulation with a temperature dependent ε_{wc} and CRU climate. We also evaluated temporal mean stem cellulose across all (European) sites. Compared to the original simulations (Fig. 4) the correlation between modeled and measured data

19

732 was slightly lower if ε_{wc} was allowed to depend on temperature ($r = 0.68$ vs. $r = 0.71$, data not

733 shown). Since we know that the CRU temperatures are too low for some sites (e.g. Fig. 7), we

734 performed an additional test where we set ε_{wc} to 31‰ to mimic the effect of low growth

735 temperatures on biochemical fractionation. This test should improve results for cool sites (INA,

736 GUT, ILO, CAV), which was indeed what we observed. For these sites the model-observation

737 differences decreased (results not shown), while for sites with high mean annual temperatures

738 (e.g. REN, LIL) LPX-Bern overestimated stem cellulose $\delta^{18}O$ or left them unchanged.

739

4 Discussion and Conclusion

741 Formulations to describe $\delta^{18}O$ in leaf water and stem cellulose are implemented in the LPX-Bern

742 DGVM and a compilation of tree ring data of $\delta^{18}O$ in stem cellulose, mainly for Europe, is

743 established. This allows us to model the large scale distribution of leaf water and stem cellulose

744 $\delta^{18}O$ on the global scale, to study spatio-temporal variability in $\delta^{18}O$, to evaluate model

745 formulations describing the transfer of $\delta^{18}O$ signals within plants, and, last but not least, to

746 investigate underlying drivers and processes. Further, the model permits us to address how inter-

747 annual, decadal and 20th century changes in climate and environmental variables may have

748 affected $\delta^{18}O$ in stem cellulose, thereby contributing to the interpretation of tree ring $\delta^{18}O$ data.

749

750 The comparison of 50-yr-averaged model results with tree ring data, mainly across Europe, shows

751 that the large scale climatological-mean pattern in stem cellulose $\delta^{18}O$ is well captured by the

752 model (Fig. 4). The high correlation between modeled time series and $\delta^{18}O$ tree ring data from

753 five sites in Switzerland suggests that the inter-annual variability in stem cellulose $\delta^{18}O$ is also

754 well represented by LPX-Bern (Fig. 5). Thus, the formulations describing water uptake by plants

755 and transpiration, regulated by stomatal conductance and influenced by ambient CO_2

756 concentrations, and corresponding isotope fractionations appear consistent with tree ring $\delta^{18}O$

757 data. In an earlier study (Saurer et al., 2014), it is shown that LPX-Bern is also able to represent

758 the spatial gradients in $\delta^{13}C$ and the temporal change in $\delta^{13}C$ and intrinsic water use efficiency

759 over the 20th century as reconstructed from a European-wide tree ring network. The good

760 agreement with tree ring data suggests that LPX-Bern is suited to explore the $\delta^{18}O$ signal transfer

20

Sonja Keel 3/2/2016 9:13 PM
Deleted: 3

Sonja Keel 3/30/2016 9:01 AM
Deleted: INA, GUT, ILO, CAV

Sonja Keel 3/2/2016 9:13 PM
Deleted: 7

Sonja Keel 3/2/2016 9:13 PM
Deleted: s

Sonja Keel 3/2/2016 9:13 PM
Deleted: 4 and 8

766 within forest ecosystems and to study the relationship between $\delta^{18}O$ in stem cellulose and

767 meteorological drivers in a mechanistic way, at least within European boreal and temperate

768 forests. This aspect may become particularly relevant in the context of global warming, with

769 more extreme conditions including heat waves and droughts expected. The model could be used

770 in future work in connection with tree ring data of growth, $\delta^{13}C$, and $\delta^{18}O$ to study the nexus

771 between flows of water (governing evaporative cooling and runoff) and C as well as C

772 sequestration. In general, we expect any changes in seasonality that could potentially affect soil

773 water $\delta^{18}O$ such as e.g. earlier snow melt to be translated to stem cellulose $\delta^{18}O$ in LPX-Bern.

774

775 Inter-annual variability and decadal scale trends of modeled tree-ring $\delta^{18}O$ in Switzerland are

776 predominantly driven by the meteorological variables relative humidity and temperature and the

777 variability in soil water and water vapor $\delta^{18}O$ (Fig. 6, Table 2). In contrast, N deposition or

778 increasing CO_2 leading to CO_2 fertilization within LPX-Bern do not influence trends and

779 variability in stem cellulose $\delta^{18}O$ at the investigated sites. This is a novel finding that is important

780 for tree-ring $\delta^{18}O$ interpretation, and contrasts with respective findings for $\delta^{13}C$, where CO_2 is an

781 important factor (Saurer et al. 2014). A strong influence of relative humidity and soil water on

782 stem cellulose $\delta^{18}O$ is consistent with expectations from isotope theory (McCarroll and Loader,

783 2004). This is also in agreement with many tree-ring studies that found a significant effect of

784 relative humidity (Burk and Stuiver, 1981), vapor pressure differences (Kahmen et al., 2011) and

785 $\delta^{18}O$ of precipitation (Waterhouse et al., 2002) based on statistical analyses. Precipitation

786 variations in our study did not influence inter-annual variability nor long-term trends in stem

787 cellulose $\delta^{18}O$ in factorial simulations where precipitation is kept constant at climatological mean

788 values. Hence, it seems unlikely that $\delta^{18}O$ as simulated by LPX-Bern will capture changes in

789 precipitation patterns that are not associated with changes in isotope signals. Nevertheless, time

790 series of precipitation at DAV are correlated with modeled time series of $\delta^{18}O$ in stem cellulose

791 (Fig. 5c) in agreement with observations (e.g. Reynolds-Henne et al., 2007; Rinne et al., 2013;

792 Hartl-Meier et al., 2015), albeit less than correlations for soil and water vapor $\delta^{18}O$ (Fig. 5b,d), air

793 temperature and humidity (Fig. 5e,f). This correlation likely arises from the impact of

794 precipitation on other variables, e.g. relative humidity, and from the correlation of precipitation

795 with other driving variables. There is clearly decadal variability in simulated stem cellulose $\delta^{18}O$

806 linked to variability in $\delta^{18}O$ and climate input data, e.g. the effect of soil water $\delta^{18}O$ varied around

807 zero in the 1960s and is consistently positive in the 1990s (Fig. 6e). The identification of potential

808 century-scale trends is hampered by the lack of suitable input data for relative humidity and $\delta^{18}O$

809 of soil water and water vapor in this study.

810 There are several sources of uncertainty that may explain the remaining deviations between

811 simulated and measured stem cellulose $\delta^{18}O$ for the Swiss and European sites. First, we run the

812 model at a coarse spatial resolution (about 220 km x 320 km in Southern Europe) and local site

813 conditions are expected to be different from grid cell average conditions. Climate input data and

814 prescribed $\delta^{18}O$ in soil water and water vapor therefore only approximate local values at the site.

815 Sensitivity simulations (Table 2) and a comparison of soil water $\delta^{18}O$ with the $\delta^{18}O$ from the

816 GNIP precipitation network reveal that uncertainties in the input data can indeed well explain

817 deviations between modeled and measured $\delta^{18}O$ in stem cellulose. Uncertainties in relative

818 humidity appear particularly relevant and are likely at the origin of relatively large data-model

819 discrepancies at humid sites. Only modest changes in humidity, and thus water pressure deficit,

820 do result in significant changes in stem cellulose $\delta^{18}O$. Daily variations and within canopy

821 variations in humidity (and other variables) are not taken into account in our approach. Second,

822 we assume that parameters such as the fractionation between water and cellulose, ε_{wc}, the path

823 length, L, for the Péclet effect or the proportion of carbonyl oxygen exchange with source water,

824 p_{ex}, are constant, although they may vary (e.g. Wang et al., 1998; Ripullone et al., 2008;

825 Sternberg and Ellsworth, 2011; Song et al., 2014). The biochemical fractionation factor ε_{wc} is

826 commonly assumed to be 27‰. Only recently Sternberg & Ellsworth (2011) suggested that ε_{wc}

827 increases up to about 31‰ at low growth temperatures of 5°C. However, their experiments were

828 performed in a rather artificial system as they studied wheat seedlings cultivated in the dark and

829 their findings are controversially discussed (Sternberg, 2014; Zech et al., 2014). Application of a

830 temperature dependent ε_{wc} in LPX-Bern in combination with meteorological data from a nearby

831 weather station removed the model-measurement offset for the alpine site DAV and improved the

832 model-measurement correlation compared to the standard setup. So far our results seem the first

833 to indicate that a temperature dependent ε_{wc} might perhaps also be relevant under field conditions.

834 Yet, uncertainties in other input data and model structure are too large to draw any firm

835 conclusions. The path length (L) of 0.03 m for the Péclet number agrees with previous studies

Sonja Keel 3/2/2016 9:20 PM
Deleted: .

Weigt Rosemarie B…, 3/29/2016 3:04 PM
Formatted: English (US)

Weigt Rosemarie B…, 3/29/2016 3:04 PM
Formatted: English (US)

Weigt Rosemarie B…, 3/29/2016 3:09 PM
Deleted: DVN

838 (Wang et al., 1998; Gessler et al., 2013), although large variability has been reported (Kahmen et
839 al., 2009). Also the proportion of carbonyl oxygen exchange with source water (p_{ex}) of 0.4 seems
840 reasonable compared with published values (Cernusak et al., 2005; Gessler et al., 2009; Gessler et
841 al., 2013; Song et al., 2014). However, relatively small changes in p_{ex} have a significant impact
842 on $\delta^{18}O$ in stem cellulose (Table 2) and recent studies suggest this value could range between 0.2
843 and 0.42 (Gessler et al., 2009; Song et al., 2014). Third, in LPX-Bern, photoassimilates are
844 allocated to growing tissues instantaneously and are not stored e.g. as starch. The simulated tree
845 ring $\delta^{18}O$ is therefore exclusively affected by the current year's meteorology, and not by that of
846 previous years.

847 The fact that soil water $\delta^{18}O$ has a strong effect on stem cellulose $\delta^{18}O$ calls for a very careful
848 evaluation of the source water input data. Unfortunately oxygen isotope ratios of soil water are
849 not systematically measured as is the case for precipitation (Global Network for Isotopes in
850 Precipitation, The GNIP Database, http://www.iaea.org/water). However, the comparison of the
851 soil water $\delta^{18}O$ data from the ECHAM5-JSBACH model as used as input to LPX-Bern with the
852 GNIP data reveal a good agreement and deviations in $\delta^{18}O$ between ECHAM5-JSBACH soil and
853 GNIP precipitation $\delta^{18}O$ data are generally less than two per mill (Haese et al. 2013).

854 Our leaf water $\delta^{18}O$ results provide another global scale estimate of leaf water $\delta^{18}O$ in addition to
855 the GIS-based approach by West et al. (2008). There are several possible reasons that could
856 explain why leaf water $\delta^{18}O$ simulated by LPX-Bern was mostly higher compared to simulations
857 by West et al. (2008) (Fig. 2). First, the $\delta^{18}O$ input data and relative humidity forcings were not
858 the same. West and colleagues used annually-averaged $\delta^{18}O$ from the GNIP precipitation
859 network, which obviously provides lower values than when summer $\delta^{18}O$ would have been used.
860 The mechanistic approach implemented in LPX-Bern considers seasonally varying $\delta^{18}O$ of both,
861 source water and atmospheric water vapor, and models explicitly daily stomatal conductance,
862 transpiration, and associated $\delta^{18}O$ transport. Second, West et al. (2008) assumed that leaf
863 temperature is 5°C higher than air temperature. Observations support this for broad-leaved, but
864 less so for needle leaved species (Leuzinger and Körner, 2007). Because sites with conifers
865 dominate our observational data set, it is reasonable to assume that leaf temperature equals air
866 temperature in our study. We only have few measurements to support this and more field data
867 would be needed for a meaningful evaluation of simulated leaf water $\delta^{18}O$. Nevertheless, the

877 LPX-Bern simulated mean value of leaf water $\delta^{18}O$ for one grid cell is within the range of the

878 mean values measured at two sites in this grid cell (Table 1). Additionally, the good agreement

879 between measured and modeled stem cellulose $\delta^{18}O$ in Europe appears to implicitly support the

880 LPX-Bern estimates in leaf water $\delta^{18}O$ for this region.

881 We implemented routines to simulate leaf water and stem cellulose $\delta^{18}O$ in the LPX-Bern DGVM

882 and successfully modeled the spatio-temporal variability in $\delta^{18}O$ as revealed by European tree

883 ring data. As tree-ring isotope networks are becoming more wide-spread, the ^{18}O-enabled LPX-

884 Bern model provides an ideal tool to explore large-scale spatial and temporal patterns in cellulose

885 $\delta^{18}O$ and to help unravel underlying processes and drivers.

886

896

897

898

899

Sonja Keel 3/29/2016 9:37 AM
Deleted: ese

Sonja Keel 3/29/2016 9:38 AM
Deleted: However

Sonja Keel 3/29/2016 9:36 AM
Deleted: more field data would be needed for a meaningful evaluation of simulated leaf water $\delta^{18}O$. T

Sonja Keel 3/2/2016 9:23 PM
Deleted: Rosi Weigt for gathering the stem cellulose $\delta^{18}O$ data across Europe,

24

References

An, W., Liu, X., Leavitt, S. W., Xu, G., Zeng, X., Wang, W., Qin, D., and Ren, J.: Relative humidity history on the Batang-Litang Plateau of western China since 1755 reconstructed from tree-ring δ^{18}O- and δ D, Climate Dynamics, 42, 2639-2654, 2014.

Anderson, W. T., Bernasconi, S. M., McKenzie, J. A., and Saurer, M.: Oxygen and carbon isotopic record of climatic variability in tree ring cellulose (*Picea abies*): An example from central Switzerland (1913-1995), Journal of Geophysical Research-Atmospheres, 103, 31625-31636, 1998.

Babst, F., Alexander, M. R., Szejner, P., Bouriaud, O., Klesse, S., Roden, J., Ciais, P., Poulter, B., Frank, D., Moore, D. J. P., and Trouet, V.: A tree-ring perspective on the terrestrial carbon cycle, Oecologia, 176, 307-322, 10.1007/s00442-014-3031-6, 2014.

Barbour, M. M., and Farquhar, G. D.: Relative humidity- and ABA-induced variation in carbon and oxygen isotope ratios of cotton leaves, Plant Cell and Environment, 23, 473-485, 2000.

Barbour, M. M., Roden, J. S., Farquhar, G. D., and Ehleringer, J. R.: Expressing leaf water and cellulose oxygen isotope ratios as enrichment above source water reveals evidence of a Péclet effect, Oecologia, 138, 426-435, 2004.

Barbour, M. M.: Stable oxygen isotope composition of plant tissue: a review, Functional Plant Biology, 34, 83-94, http://dx.doi.org/10.1071/FP06228, 2007.

Begert, M., Schlegel, T., and Kirchhofer, W.: Homogeneous temperature and precipitation series of Switzerland from 1864 to 2000, International Journal of Climatology, 25, 65-80, doi:10.1002/joc.1118/abstract, 2005.

Bottinga, Y., and Craig, H.: Oxygen isotope fractionation between CO_2 and water and isotopic composition of marine atmospheric CO_2, Earth and Planetary Science Letters, 5, 285-295, 1969.

Bowen, G. J., and Revenaugh, J.: Interpolating the isotopic composition of modern meteoric precipitation, Water Resources Research, 39, 1299, 2003.

Burk, R. L., and Stuiver, M.: Oxygen isotope ratios in trees reflect mean annual temperature and humidity, Science, 211, 1417-1419, 1981.

Cappa, C. D., Hendricks, M. B., DePaolo, D. J., and Cohen, R. C.: Isotopic fractionation of water during evaporation, Journal of Geophysical Research: Atmospheres, 108, 1-10, 10.1029/2003jd003597, 2003.

Cernusak, L. A., Farquhar, G. D., and Pate, J. S.: Environmental and physiological controls over oxygen and carbon isotope composition of Tasmanian blue gum, *Eucalyptus globulus*, Tree Physiology, 25, 129-146, 2005.

Collatz, G. J., Ball, J. T., Grivet, C., and Berry, J. A.: Physiological and environmental regulation of stomatal conductance, photosynthesis and transpiration - A model that includes a laminar boundary layer, Agricultural and Forest Meteorology, 54, 107-136, 1991.

Collatz, G. J., Ribas-Carbo, M., and Berry, J. A.: Coupled photosynthesis-stomatal conductance model for leaves of C_4 plants, Australian Journal of Plant Physiology, 19, 519-538, 1992.

25

Craig, H., and Gordon, L.: Deuterium and oxygen 18 variations in the ocean and the marine atmosphere, Consiglio Nazionale delle Ricerche, Laboratorio di Geologia Nucleare, Pisa, 1965.

Cuntz, M., Ogée, J., Farquhar, G. D., Peylin, P., and Cernusak, L. A.: Modelling advection and diffusion of water isotopologues in leaves, Plant, Cell & Environment, 30, 892-909, 10.1111/j.1365-3040.2007.01676.x, 2007.

Dansgaard, W.: Stable isotopes in precipitation, Tellus A, 16, 10.3402/tellusa.v16i4.8993, 1964.

Dongmann, G., Nürnberg, H. W., Förstel, H., and Wagener, K.: On the enrichment of $H_2^{18}O$ in the leaves of transpiring plants, Radiation and Environmental Biophysics, 11, 41-52, 10.1007/BF01323099, 1974.

Dunbar, R. B., Wellington, G. M., Colgan, M. W., and Glynn, P. W.: Eastern Pacific sea-surface temperature since 1600 A.D.: The $\delta^{18}O$ record of climate variability in Galápagos corals, Paleoceanography, 9, 291-315, 1994.

Edwards, T. W. D., Birks, S. J., Luckman, B. H., and MacDonald, G. M.: Climatic and hydrologic variability during the past millennium in the eastern Rocky Mountains and northern Great Plains of western Canada, Quaternary Research, 70, 188-197, dx.doi.org/10.1016/j.yqres.2008.04.013, 2008.

Elderfield, H., and Ganssen, G.: Past temperature and $\delta^{18}O$ of surface ocean waters inferred from foraminiferal Mg/Ca ratios, Nature, 405, 442-445, 2000.

Epstein, S., Thompson, P., and Yapp, C. J.: Oxygen and hydrogen isotopic ratios in plant cellulose, Science, 198, 1209-1215, 1977.

Etheridge, D. M., Steele, L. P., Langenfelds, R. L., Francey, R. J., Barnola, J. M., and Morgan, V. I.: Historical CO_2 records from the Law Dome DE08, DE08-2, and DSS ice cores, in: Trends: A Compendium of Data on Global Change. Carbon Dioxide Information Analysis Center, Oak Ridge National Laboratory, U.S. Department of Energy http://cdiac.ornl.gov/trends/co2/lawdome.html, Oak Ridge, Tenn., U.S.A, 1998.

Farquhar, G. D., von Caemmerer, S., and Berry, J. A.: A biochemical model of photosynthetic CO_2 assimilation in leaves of C_3 species, Planta, 149, 78-90, 1980.

Farquhar, G. D., and von Caemmerer, S.: Modelling of photosynthetic response to environmental conditions, in: Physiological Plant Ecology II: Water Relations and Carbon Assimilation, edited by: Nobel, P. S., Osmond, C. B., and Ziegler, H., Spriner, Berlin, 549-587, 1982.

Farquhar, G. D., and Lloyd, J.: Carbon and oxygen isotope effects in the exchange of carbon dioxide between terrestrial plants and the atmosphere., in: Stable isotopes and plant carbon–water relations, edited by: Ehleringer, J. R., Hall, A. E., and Farquhar, G. D., Academic Press, San Diego, 47–70, 1993.

Farquhar, G. D., and Gan, K. S.: On the progressive enrichment of the oxygen isotopic composition of water along a leaf, Plant Cell and Environment, 26, 1579-1597, 2003.

Ferrio, J. P., and Voltas, J.: Carbon and oxygen isotope ratios in wood constituents of *Pinus halepensis* as indicators of precipitation, temperature and vapour pressure deficit, Tellus Series B-Chemical and Physical Meteorology, 57, 164-173, 2005.

26

986 Flanagan, L. B., Comstock, J. P., and Ehleringer, J. R.: Comparison of Modeled and Observed
987 Environmental Influences on the Stable Oxygen and Hydrogen Isotope Composition of Leaf
988 Water in *Phaseolus vulgaris* L., Plant Physiology, 96, 588-596, 1991.

989 Fleitmann, D., Burns, S. J., Neff, U., Mudelsee, M., Mangini, A., and Matter, A.: Palaeoclimatic
990 interpretation of high-resolution oxygen isotope profiles derived from annually laminated
991 speleothems from Southern Oman, Quaternary Science Reviews, 23, 935-945,
992 10.1016/j.quascirev.2003.06.019, 2004.

993 Gerten, D., Schaphoff, S., Haberlandt, U., Lucht, W., and Sitch, S.: Terrestrial vegetation and
994 water balance - hydrological evaluation of a dynamic global vegetation model, Journal of
995 Hydrology, 286, 249-270, 2004.

996 Gessler, A., Keitel, C., Kodama, N., Weston, C., Winters, A. J., Keith, H., Grice, K., Leuning, R.,
997 and Farquhar, G. D.: δ^{13}C of organic matter transported from the leaves to the roots in *Eucalyptus*
998 *delegatensis*: short-term variations and relation to respired CO_2, Functional Plant Biology, 34,
999 692-706, 10.1071/fp07064, 2007.

1000 Gessler, A., Brandes, E., Buchmann, N., Helle, G., Rennenberg, H., and Barnard, R. L.: Tracing
1001 carbon and oxygen isotope signals from newly assimilated sugars in the leaves to the tree-ring
1002 archive, Plant Cell and Environment, 32, 780-795, 2009.

1003 Gessler, A., Brandes, E., Keitel, C., Boda, S., Kayler, Z. E., Granier, A., Barbour, M., Farquhar,
1004 G. D., and Treydte, K.: The oxygen isotope enrichment of leaf-exported assimilates - does it
1005 always reflect lamina leaf water enrichment?, New Phytologist, 200, 144-157, 2013.

1006 Gessler, A., Pedro Ferrio, J., Hommel, R., Treydte, K., Werner, R. A., and Monson, R. K.: Stable
1007 isotopes in tree rings: towards a mechanistic understanding of isotope fractionation and mixing
1008 processes from the leaves to the wood, Tree Physiology, 34, 796-818, 2014.

1009 Haese, B., Werner, M., and Lohmann, G.: Stable water isotopes in the coupled atmosphere–land
1010 surface model ECHAM5-JSBACH, Geosci. Model Dev., 6, 1463-1480, 10.5194/gmd-6-1463-
1011 2013, 2013.

1012 Harris, I., Jones, P. D., Osborn, T. J., and Lister, D. H.: Updated high-resolution grids of monthly
1013 climatic observations - the CRU TS3.10 Dataset, International Journal of Climatology, 34, 623-
1014 642, 2014.

1015 Hartl-Meier, C., Zang, C., Buentgen, U., Esper, J., Rothe, A., Goettlein, A., Dirnboeck, T., and
1016 Treydte, K.: Uniform climate sensitivity in tree-ring stable isotopes across species and sites in a
1017 mid-latitude temperate forest, Tree Physiology, 35, 4-15, 2015.

1018 Haxeltine, A., and Prentice, I. C.: A general model for the light-use efficiency of primary
1019 production, Functional Ecology, 10, 551-561, 1996a.

1020 Haxeltine, A., and Prentice, I. C.: BIOME3: An equilibrium terrestrial biosphere model based on
1021 ecophysiological constraints, resource availability, and competition among plant functional types,
1022 Global Biogeochemical Cycles, 10, 693-709, 1996b.

1023 Herweijer, C., Seager, R., Cook, E. R., and Emile-Geay, J.: North American droughts of the last
1024 millennium from a gridded network of tree-ring data, Journal of Climate, 20, 1353-1376, 2007.

27

Hoffmann, G., Werner, M., and Heimann, M.: Water isotope module of the ECHAM atmospheric general circulation model: A study on timescales from days to several years, Journal of Geophysical Research-Atmospheres, 103, 16871-16896, 1998.

Hoffmann, G., Ramirez, E., Taupin, J. D., Francou, B., Ribstein, P., Delmas, R., Durr, H., Gallaire, R., Simoes, J., Schotterer, U., Stievenard, M., and Werner, M.: Coherent isotope history of Andean ice cores over the last century, Geophysical Research Letters, 30, 1179, 2003.

Johnsen, S. J., Dahl-Jensen, D., Gundestrup, N., Steffensen, J. P., Clausen, H. B., Miller, H., Masson-Delmotte, V., Sveinbjörnsdottir, A. E., and White, J.: Oxygen isotope and palaeotemperature records from six Greenland ice-core stations: Camp Century, Dye-3, GRIP, GISP2, Renland and NorthGRIP, Journal of Quaternary Science, 16, 299-307, 10.1002/jqs.622, 2001.

Joussaume, S., Sadourny, R., and Jouzel, J.: A general circulation model of water isotope cycles in the atmosphere, Nature, 311, 24-29, 1984.

Jouzel, J., Russell, G. L., Suozzo, R. J., Koster, R. D., White, J. W. C., and Broecker, W. S.: Simulations of the HDO and H_2O^{18} atmospheric cycles using the NASA GISS general-circulation model - The seasonal cycle for present-day conditions, Journal of Geophysical Research-Atmospheres, 92, 14739-14760, 1987.

Jouzel, J., Vimeux, F., Caillon, N., Delaygue, G., Hoffmann, G., Masson-Delmotte, V., and Parrenin, F.: Magnitude of isotope/temperature scaling for interpretation of central Antarctic ice cores, Journal of Geophysical Research-Atmospheres, 108, 4361, 2003.

Kahmen, A., Simonin, K., Tu, K., Goldsmith, G. R., and Dawson, T. E.: The influence of species and growing conditions on the 18-O enrichment of leaf water and its impact on 'effective path length', New Phytologist, 184, 619-630, 10.1111/j.1469-8137.2009.03008.x, 2009.

Kahmen, A., Sachse, D., Arndt, S. K., Tu, K. P., Farrington, H., Vitousek, P. M., and Dawson, T. E.: Cellulose $\delta^{18}O$ is an index of leaf-to-air vapor pressure difference (VPD) in tropical plants, Proceedings of the National Academy of Sciences of the United States of America, 108, 1981-1986, 10.1073/pnas.1018906108, 2011.

Kearney, M. R., Isaac, A. P., and Porter, W. P.: microclim: Global estimates of hourly microclimate based on long-term monthly climate averages, Scientific Data, 1, 2014.

Kern, Z., Kohan, B., and Leuenberger, M.: Precipitation isoscape of high reliefs: interpolation scheme designed and tested for monthly resolved precipitation oxygen isotope records of an Alpine domain, Atmospheric chemistry and physics, 14, 1897-1907, 2014.

Kress, A., Saurer, M., Siegwolf, R. T. W., Frank, D. C., Esper, J., and Bugmann, H.: A 350 year drought reconstruction from Alpine tree ring stable isotopes, Global Biogeochemical Cycles, 24, GB2011, 2010.

Lamarque, J.-F., Kyle, G. P., Meinshausen, M., Riahi, K., Smith, S. J., van Vuuren, D. P., Conley, A. J., and Vitt, F.: Global and regional evolution of short-lived radiatively-active gases and aerosols in the Representative Concentration Pathways, Climatic Change, 109, 191-212, 2011.

Sonja Keel 3/28/2016 3:16 PM
Deleted: .

Weigt Rosemarie B…, 3/29/2016 3:04 PM
Formatted: English (US)

28

1065 Leuzinger, S., and Körner, C.: Tree species diversity affects canopy leaf temperatures in a mature
1066 temperate forest, Agricultural and Forest Meteorology, 146, 29-37, 2007.

1067 Libby, L. M., Pandolfi, L. J., Payton, P. H., Marshall, J., Becker, B., and Giertz-Sienbenlist, V.:
1068 Isotopic tree thermometers, Nature, 261, 284-288, 10.1038/261284a0, 1976.

1069 MacFarling Meure, C., Etheridge, D., Trudinger, C., Steele, P., Langenfelds, R., van Ommen, T.,
1070 Smith, A., and Elkins, J.: Law Dome CO_2, CH_4 and N_2O ice core records extended to 2000 years
1071 BP, Geophysical Research Letters, 33, L14810, 2006.

1072 Masson-Delmotte, V., Raffalli-Delerce, G., Danis, P. A., Yiou, P., Stievenard, M., Guibal, F.,
1073 Mestre, O., Bernard, V., Goosse, H., Hoffmann, G., and Jouzel, J.: Changes in European
1074 precipitation seasonality and in drought frequencies revealed by a four-century-long tree-ring
1075 isotopic record from Brittany, western France, Climate Dynamics, 24, 57-69, 2005.

1076 Masson-Delmotte, V., Steen-Larsen, H. C., Ortega, P., Swingedouw, D., Popp, T., Vinther, B.
1077 M., Oerter, H., Sveinbjornsdottir, A. E., Gudlaugsdottir, H., Box, J. E., Falourd, S., Fettweis, X.,
1078 Gallée, H., Garnier, E., Gkinis, V., Jouzel, J., Landais, A., Minster, B., Paradis, N., Orsi, A., Risi,
1079 C., Werner, M., and White, J. W. C.: Recent changes in north-west Greenland climate
1080 documented by NEEM shallow ice core data and simulations, and implications for past-
1081 temperature reconstructions, The Cryosphere, 9, 1481-1504, 10.5194/tc-9-1481-2015, 2015.

1082 McCarroll, D., and Loader, N. J.: Stable isotopes in tree rings, Quaternary Science Reviews, 23,
1083 771-801, 10.1016/j.quascirev.2003.06.017, 2004.

1084 McDermott, F.: Palaeo-climate reconstruction from stable isotope variations in speleothems: a
1085 review, Quaternary Science Reviews, 23, 901-918, 10.1016/j.quascirev.2003.06.021, 2004.

1086 Miller, D. L., Mora, C. I., Grissino-Mayer, H. D., Mock, C. J., Uhle, M. E., and Sharp, Z.: Tree-
1087 ring isotope records of tropical cyclone activity, Proceedings of the National Academy of
1088 Sciences, 103, 14294-14297, 10.1073/pnas.0606549103, 2006.

1089 Monteith, J. L.: A Reinterpretation of Stomatal Responses to Humidity, Plant, Cell and
1090 Environment, 18, 357-364, 1995.

1091 Murray, S. J., Foster, P. N., and Prentice, I. C.: Evaluation of global continental hydrology as
1092 simulated by the Land-surface Processes and eXchanges Dynamic Global Vegetation Model,
1093 Hydrology and Earth System Sciences, 15, 91-105, 2011.

1094 Noone, D., and Simmonds, I.: Associations between $\delta^{18}O$ of water and climate parameters in a
1095 simulation of atmospheric circulation for 1979-95, Journal of Climate, 15, 3150-3169, 2002.

1096 Offermann, C., Pedro Ferrio, J., Holst, J., Grote, R., Siegwolf, R., Kayler, Z., and Gessler, A.:
1097 The long way down-are carbon and oxygen isotope signals in the tree ring uncoupled from
1098 canopy physiological processes?, Tree Physiology, 31, 1088-1102, 2011.

1099 Ogée, J., Barbour, M. M., Wingate, L., Bert, D., Bosc, A., Stievenard, M., Lambrot, C., Pierre,
1100 M., Bariac, T., Loustau, D., and Dewar, R. C.: A single-substrate model to interpret intra-annual
1101 stable isotope signals in tree-ring cellulose, Plant Cell and Environment, 32, 1071-1090, 2009.

1102 Prentice, I. C., Kelley, D. I., Foster, P. N., Friedlingstein, P., Harrison, S. P., and Bartlein, P. J.:
1103 Modeling fire and the terrestrial carbon balance, Global Biogeochemical Cycles, 25, GB3005,
1104 2011.

Raddatz, T. J., Reick, C. H., Knorr, W., Kattge, J., Roeckner, E., Schnur, R., Schnitzler, K. G., Wetzel, P., and Jungclaus, J.: Will the tropical land biosphere dominate the climate-carbon cycle feedback during the twenty-first century?, Climate Dynamics, 29, 565-574, 2007.

Reynolds-Henne, C. E., Siegwolf, R. T. W., Treydte, K. S., Esper, J., Henne, S., and Saurer, M.: Temporal stability of climate-isotope relationships in tree rings of oak and pine (Ticino, Switzerland), Global Biogeochemical Cycles, 21, 2007.

Rinne, K. T., Loader, N. J., Switsur, V. R., and Waterhouse, J. S.: 400-year May-August precipitation reconstruction for Southern England using oxygen isotopes in tree rings, Quaternary Science Reviews, 60, 13-25, 2013.

Ripullone, F., Matsuo, N., Stuart-Williams, H., Wong, S. C., Borghetti, M., Tani, M., and Farquhar, G.: Environmental Effects on Oxygen Isotope Enrichment of Leaf Water in Cotton Leaves, Plant Physiology, 146, 729-736, 2008.

Risi, C., Bony, S., Vimeux, F., and Jouzel, J.: Water-stable isotopes in the LMDZ4 general circulation model: Model evaluation for present-day and past climates and applications to climatic interpretations of tropical isotopic records, Journal of Geophysical Research-Atmospheres, 115, D12118, 2010.

Roden, J. S., Lin, G. G., and Ehleringer, J. R.: A mechanistic model for interpretation of hydrogen and oxygen isotope ratios in tree-ring cellulose, Geochimica Et Cosmochimica Acta, 64, 21-35, 10.1016/S0016-7037(99)00195-7, 2000.

Roeckner, E., Bäuml, G., Bonaventura, L., Brokopf, R., Esch, M., Giorgetta, M., Hagemann, S., Kirchner, I., Kornblueh, L., Manzini, E., Rhodin, A., Schlese, U., Schulzweida, U., and Tompkins, A.: The atmospheric general circulation model ECHAM5 - Part 1, Max-Planck-Institut für Meteorologie, Report No. 349, 2003.

Rozanski, K., Araguasaraguas, L., and Gonfiantini, R.: Relation between long-term trends of ^{18}O isotope composition of precipitation and climate, Science, 258, 981-985, 1992.

Ruosch, M., Spahni, R., Joos, F., Henne, P. D., van der Knaap, P., and Tinner, W.: Past and future evolution of *Abies alba* forests in Europe – comparison of a dynamic vegetation model with palaeo data and observations, Global Change Biology, 22, 727-740, 2016.

Sarris, D., Siegwolf, R., and Körner, C.: Inter- and intra-annual stable carbon and oxygen isotope signals in response to drought in Mediterranean pines, Agricultural and Forest Meteorology, 168, 59-68, 2013.

Saurer, M., Schweingruber, F., Vaganov, E. A., Shiyatov, S. G., and Siegwolf, R.: Spatial and temporal oxygen isotope trends at the northern tree-line in Eurasia, Geophysical Research Letters, 29, 7-1, 10.1029/2001GL013739, 2002.

Saurer, M., Spahni, R., Frank, D. C., Joos, F., Leuenberger, M., Loader, N. J., McCarroll, D., Gagen, M., Poulter, B., Siegwolf, R. T. W., Andreu-Hayles, L., Boettger, T., Dorado Linan, I., Fairchild, I. J., Friedrich, M., Gutierrez, E., Haupt, M., Hilasvuori, E., Heinrich, I., Helle, G., Grudd, H., Jalkanen, R., Levanic, T., Linderholm, H. W., Robertson, I., Sonninen, E., Treydte, K., Waterhouse, J. S., Woodley, E. J., Wynn, P. M., and Young, G. H. F.: Spatial variability and temporal trends in water-use efficiency of European forests, Global Change Biology, 20, 3700-3712, 2014.

30

Schär, C., Vidale, P. L., Lüthi, D., Frei, C., Häberli, C., Liniger, M. A., and Appenzeller, C.: The role of increasing temperature variability in European summer heatwaves, Nature, 427, 332-336, 2004.

Severinghaus, J. P., Beaudette, R., Headly, M. A., Taylor, K., and Brook, E. J.: Oxygen-18 of O_2 Records the Impact of Abrupt Climate Change on the Terrestrial Biosphere, Science, 324, 1431-1434, 2009.

Shackleton, N. J., and Obdyke, N. D.: Oxygen-isotope and paleomagnetic stratigraphy of equatorial Pacific core V28–238: oxygen-isotope temperatures and ice volumes on an 10^5 year to 10^6 year scale, Quaternary Research, 3, 39-55, 1973.

Sidorova, O. V., Siegwolf, R. T. W., Saurer, M., Naurzbaev, M. M., and Vaganov, E. A.: Isotopic composition ($\delta^{13}C$, $\delta^{18}O$) in wood and cellulose of Siberian larch trees for early Medieval and recent periods, Journal of Geophysical Research-Biogeosciences, 113, G02019, 2008.

Sitch, S., Smith, B., Prentice, I. C., Arneth, A., Bondeau, A., Cramer, W., Kaplan, J. O., Levis, S., Lucht, W., Sykes, M. T., Thonicke, K., and Venevsky, S.: Evaluation of ecosystem dynamics, plant geography and terrestrial carbon cycling in the LPJ dynamic global vegetation model, Global Change Biology, 9, 161-185, 10.1046/j.1365-2486.2003.00569.x, 2003.

Sjolte, J., Hoffmann, G., Johnsen, S. J., Vinther, B. M., Masson-Delmotte, V., and Sturm, C.: Modeling the water isotopes in Greenland precipitation 1959–2001 with the meso-scale model REMO-iso, Journal of Geophysical Research: Atmospheres, 116, 1-22, 10.1029/2010jd015287, 2011.

Song, X., Clark, K. S., and Helliker, B. R.: Interpreting species-specific variation in tree-ring oxygen isotope ratios among three temperate forest trees, Plant, Cell & Environment, 37, 2169-2182, 2014.

Spahni, R., Joos, F., Stocker, B. D., Steinacher, M., and Yu, Z. C.: Transient simulations of the carbon and nitrogen dynamics in northern peatlands: from the Last Glacial Maximum to the 21st century, Clim. Past, 9, 1287-1308, 10.5194/cp-9-1287-2013, 2013.

Sternberg, L., and Ellsworth, P. F. V.: Divergent Biochemical Fractionation, Not Convergent Temperature, Explains Cellulose Oxygen Isotope Enrichment across Latitudes, PLoS ONE, 6, e28040, 2011.

Sternberg, L. d. S. L., DeNiro, M. J., and Savidge, R. A.: Oxygen Isotope Exchange between Metabolites and Water during Biochemical Reactions Leading to Cellulose Synthesis, Plant Physiology, 82, 423-427, 1986.

Sternberg, L. d. S. L.: Comment on "Oxygen isotope ratios ($^{18}O/^{16}O$) of hemicellulose-derived sugar biomarkers in plants, soils and sediments as paleoclimate proxy I: Insight from a climate chamber experiment" by Zech et al. (2014), Geochimica Et Cosmochimica Acta, 141, 677-679, 2014.

Sternberg, L. d. S. L. O. R.: Oxygen stable isotope ratios of tree-ring cellulose: the next phase of understanding, New Phytologist, 181, 553-562, 10.1111/j.1469-8137.2008.02661.x, 2009.

Weigt Rosemarie B…, 3/29/2016 3:04 PM
Formatted: English (US)

31

Stocker, B. D., Roth, R., Joos, F., Spahni, R., Steinacher, M., Zaehle, S., Bouwman, L., Xu, R., and Prentice, I. C.: Multiple greenhouse-gas feedbacks from the land biosphere under future climate change scenarios, Nature Climate Change, 3, 666-672, 2013.

Sturm, K., Hoffmann, G., Langmann, B., and Stichler, W.: Simulation of δ^{18}O in precipitation by the regional circulation model REMO$_{iso}$, Hydrological Processes, 19, 3425–3444, 10.1002/hyp.5979, 2005.

Treydte, K., Frank, D., Esper, J., Andreu, L., Bednarz, Z., Berninger, F., Boettger, T., D'Alessandro, C. M., Etien, N., Filot, M., Grabner, M., Guillemin, M. T., Gutierrez, E., Haupt, M., Helle, G., Hilasvuori, E., Jungner, H., Kalela-Brundin, M., Krapiec, M., Leuenberger, M., Loader, N. J., Masson-Delmotte, V., Pazdur, A., Pawelczyk, S., Pierre, M., Planells, O., Pukiene, R., Reynolds-Henne, C. E., Rinne, K. T., Saracino, A., Saurer, M., Sonninen, E., Stievenard, M., Switsur, V. R., Szczepanek, M., Szychowska-Krapiec, E., Todaro, L., Waterhouse, J. S., Weigl, M., and Schleser, G. H.: Signal strength and climate calibration of a European tree-ring isotope network, Geophysical Research Letters, 34, 2007.

Treydte, K., Boda, S., Pannatier, E. G., Fonti, P., Frank, D., Ullrich, B., Saurer, M., Siegwolf, R., Battipaglia, G., Werner, W., and Gessler, A.: Seasonal transfer of oxygen isotopes from precipitation and soil to the tree ring: source water versus needle water enrichment, New Phytologist, 202, 772-783, 2014.

Treydte, K. S., Schleser, G. H., Helle, G., Frank, D. C., Winiger, M., Haug, G. H., and Esper, J.: The twentieth century was the wettest period in northern Pakistan over the past millennium, Nature, 440, 1179-1182, 10.1038/nature04743, 2006.

Wang, X. F., Yakir, D., and Avishai, M.: Non-climatic variations in the oxygen isotopic compositions of plants, Global Change Biology, 4, 835-849, 1998.

Wania, R., Ross, I., and Prentice, I. C.: Integrating peatlands and permafrost into a dynamic global vegetation model: 2. Evaluation and sensitivity of vegetation and carbon cycle processes, Global Biogeochemical Cycles, 23, GB3015, 2009.

Waterhouse, J. S., Switsur, V. R., Barker, A. C., Carter, A. H. C., and Robertson, I.: Oxygen and hydrogen isotope ratios in tree rings: how well do models predict observed values?, Earth and Planetary Science Letters, 201, 421-430, 10.1016/S0012-821X(02)00724-0, 2002.

Weigt, R. B., Bräunlich, S., Zimmermann, L., Saurer, M., Grams, T. E. E., Dietrich, H.-P., Siegwolf, R. T. W., Nikolova, P. S.: Comparison of δ^{18}O and δ^{13}C values between tree-ring whole wood and cellulose in five species growing under two different site conditions, Rapid Communications in Mass Spectrometry, 29, 2233–2244, 2015.

Werner, M., Langebroek, P. M., Carlsen, T., Herold, M., and Lohmann, G.: Stable water isotopes in the ECHAM5 general circulation model: Toward high-resolution isotope modeling on a global scale, Journal of Geophysical Research-Atmospheres, 116, D15109, 2011.

Wershaw, R. L., Friedman, I., Heller, S. J., and Frank, P. A.: Hydrogen isotope fractionation of water passing through trees, in: Advances in organic geochemistry, edited by: Hobson, G. D., Pergamon Press, Oxford, 55-67, 1966.

West, J. B., Sobek, A., and Ehleringer, J. R.: A Simplified GIS Approach to Modeling Global Leaf Water Isoscapes, PLoS ONE, 3, e2447, 2008.

Sonja Keel 3/30/2016 9:08 AM
Formatted ... [11]

Sonja Keel 3/30/2016 9:10 AM
Deleted: .

Sonja Keel 3/30/2016 9:10 AM
Deleted: 2015.

Sonja Keel 3/30/2016 9:08 AM
Formatted: Font:12 pt

Sonja Keel 3/30/2016 9:08 AM
Formatted ... [12]

Sonja Keel 3/30/2016 9:12 AM
Deleted: .

Sonja Keel 3/30/2016 9:08 AM
Formatted ... [13]

Sonja Keel 3/30/2016 9:10 AM
Deleted: :

Sonja Keel 3/30/2016 9:10 AM
Formatted: Font:12 pt

Sonja Keel 3/30/2016 9:11 AM
Deleted: .

Sonja Keel 3/30/2016 9:08 AM
Formatted ... [14]

1234 Xu, G., Liu, X., Qin, D., Chen, T., Wang, W., Wu, G., Sun, W., An, W., and Zeng, X.: Relative
1235 humidity reconstruction for northwestern China's Altay Mountains using tree-ring $\delta^{18}O$, Chinese
1236 Science Bulletin, 59, 190-200, 2014.

1237 Zech, M., Mayr, C., Tuthorn, M., Leiber-Sauheitl, K., and Glaser, B.: Reply to the comment of
1238 Sternberg on "Zech et al. (2014) Oxygen isotope ratios ($^{18}O/^{16}O$) of hemicellulose-derived sugar
1239 biomarkers in plants, soils and sediments as paleoclimate proxy I: Insight from a climate chamber
1240 experiment. GCA 126, 614-623.", Geochimica Et Cosmochimica Acta, 141, 680-682, 2014.

1241
1242

1243 Table 1. Comparison of input data and simulations by LPX-Bern (Model) against measurements
1244 (Observed) performed at two sites (LOV, LOT) in the Lötschen Valley (Switzerland) for
1245 averages across June, July, and August 2008. Because the two sites lie within the same grid cell
1246 of LPX-Bern, the simulated data are identical.

1247

Parameter	Observed		Model
	LOV	LOT	LPX-Bern
Air temperature [°C]	15.4	11.1	16.5
Relative humidity [%]	75.6	72.6	78.5
Precipitation [mm]	251.5	294.8	387.0
Soil water $\delta^{18}O$ [‰]	-6.1	-8.6	-7.8
Needle water $\delta^{18}O$ [‰]	10.6	3.0	6.5
Stem cellulose $\delta^{18}O$ [‰]	29.2	29.0	27.3
Enrichment of needle water above source [‰]	16.7	11.6	14.3
Enrichment of stem cellulose above needle water [‰]	18.6	26.0	20.8
Enrichment of stem cellulose above source [‰]	35.3	37.6	35.1

1248
1249

34

1250   Table 2. Effect of a 10% increase in parameter values/input data on simulated stem cellulose $\delta^{18}O$

1251   at site DAV for the June, July, and August 1960 average.

1252

Parameter	Change in stem cellulose $\delta^{18}O$ [‰]
Air temperature [ºC]	-0.2
Relative humidity	-6.7
ε_k	1.7
ε^+	2.3
Transpiration (E)	-0.3
Path length (L)	-0.3
Péclet number ($\wp$)	-0.3
p_{ex}	-1.9
$\delta^{18}O_{sw}$	2.4
$\delta^{18}O_{wv}$	2.9

1253

1254

Soil water δ^{18}O ($^o/_{oo}$)

Water vapor δ^{18}O ($^o/_{oo}$)
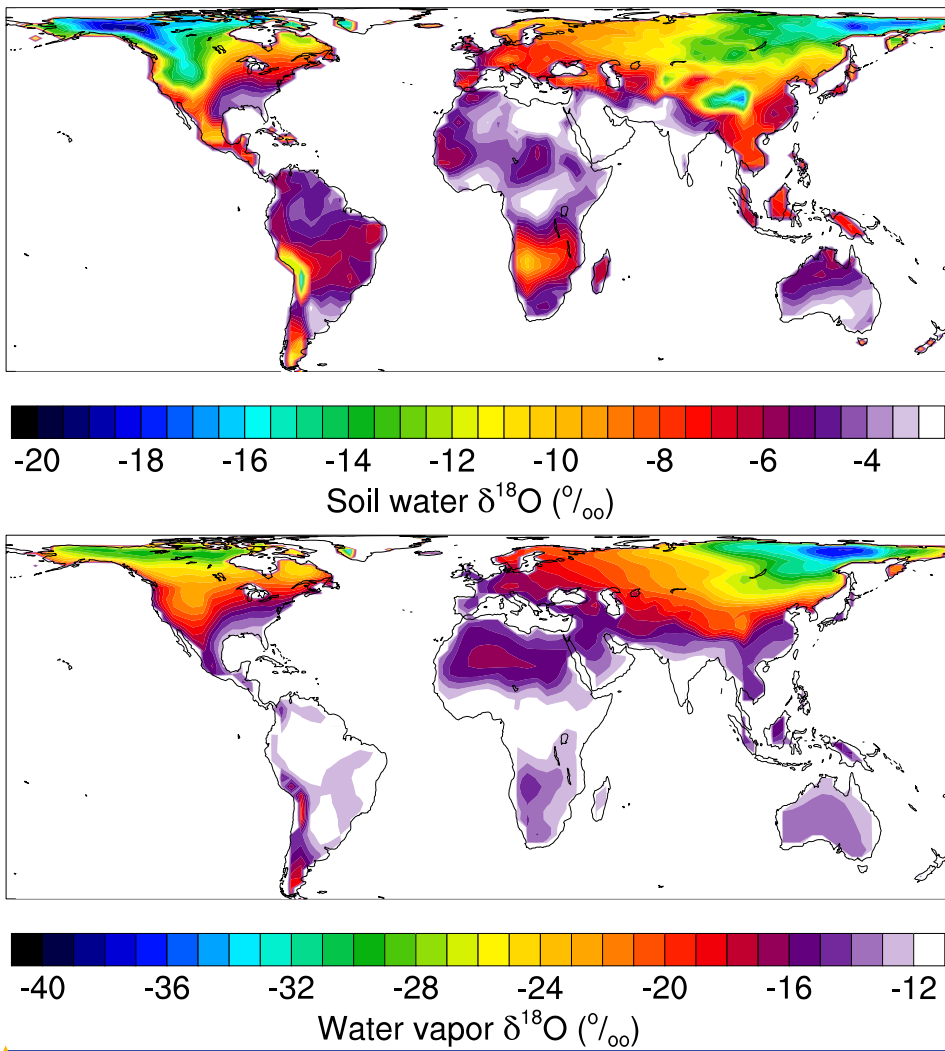
1256

1257 Figure 1. Simulated monthly soil water δ^{18}O (upper panel) and water vapor δ^{18}O (lower panel)
1258 was used as input data for the calculation of leaf water and cellulose δ^{18}O by LPX-Bern. The
1259 presented data were simulated by the coupled atmosphere-land surface model ECHAM5-
1260 JSBACH (Haese et al. 2013). Average values for 1961-1990 are shown.
1261
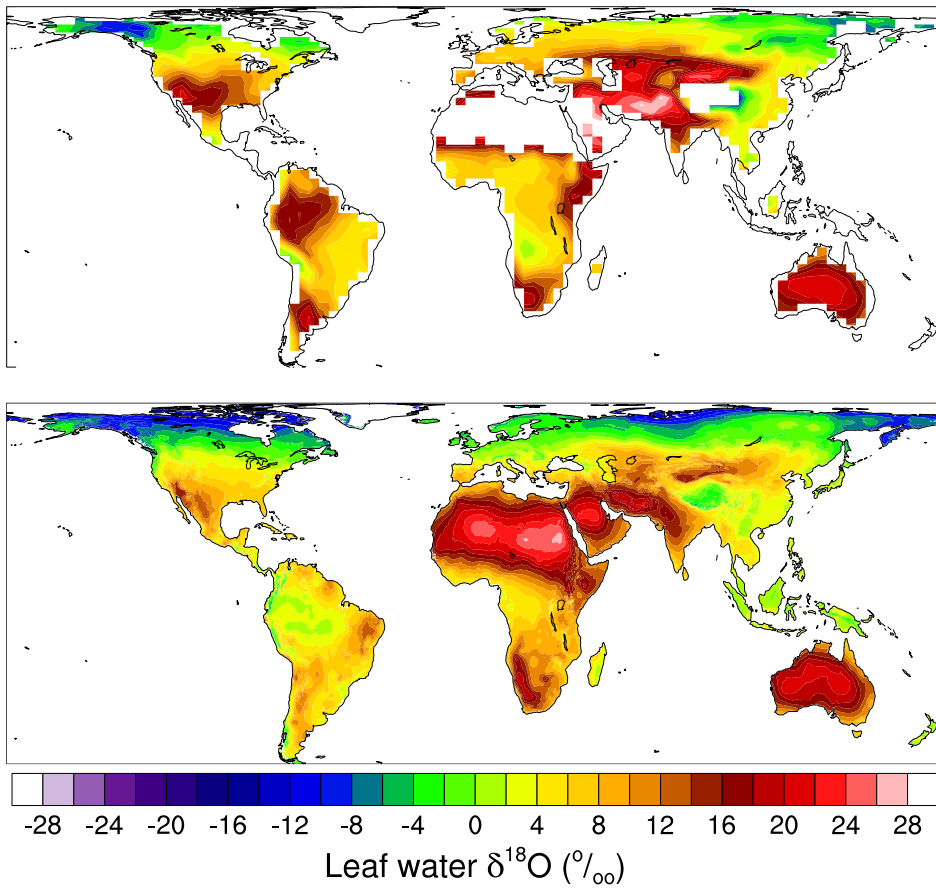
1263

1264 Figure 2. Leaf water $\delta^{18}O$ (‰) as simulated by LPX-Bern (upper panel) compared to results by

1265 West et al. (2008) using a GIS approach (lower panel). LPX-Bern results are shown for the years

1266 1961-1990 using the Craig-Gordon formulation (i.e. no Péclet effect) for comparability and for all

1267 plant functional types including grasses and herbs.

1268

1269

1270

1271

a

Leaf water-soil water $\delta^{18}O$ ($^o/_{oo}$)

10 12 14 16 18 20 22 24 26 28 30

b

Stem cellulose $\delta^{18}O$ ($^o/_{oo}$)

15 17 19 21 23 25 27 29 31 33 35
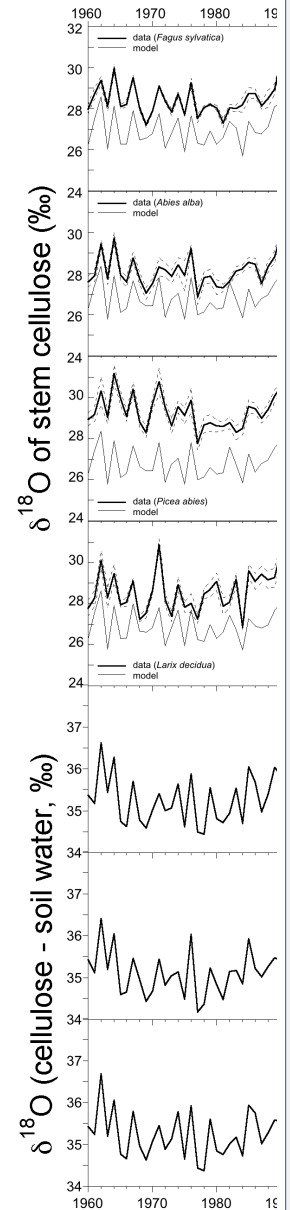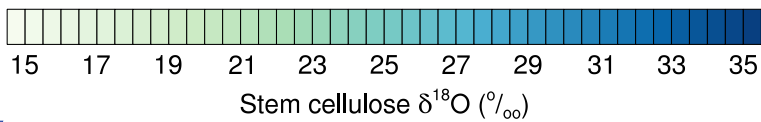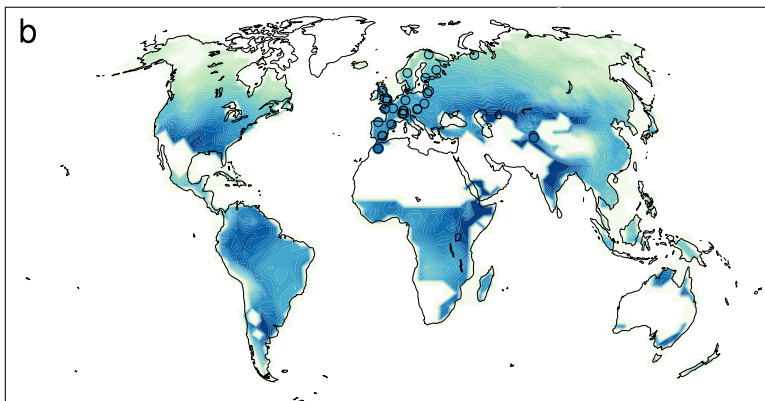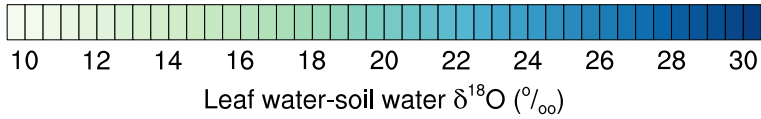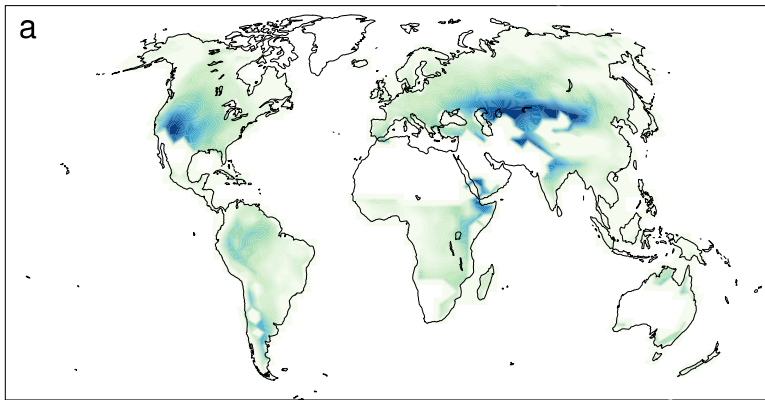
Figure 3. Leaf water ^{18}O enrichment above soil water $\delta^{18}O$ (a) and stem cellulose $\delta^{18}O$ (b) averaged over all tree plant functional types and over 1961-2012 as simulated by LPX-Bern. Colored circles in panel b show temporally-averaged results from local tree ring data (Table S1 in the Supplement) on the same color scale as model results.

38

$$y = 0.78x + 4.9, \; r = 0.71^{***}$$

● high RH (%)
○ low biomass

1317

1318 Figure 4. Comparison of simulated and measured stem cellulose $\delta^{18}O$ for 31 sites in temperate
1319 and boreal forests (mainly in Europe). Each symbol represents the mean over the years 1960-
1320 2003 (or up to 2012 if available) for a specific species (e.g. *Quercus petraea* (Matt.) Liebl., Table
1321 S1) and the corresponding plant functional type in LPX-Bern. Sites where the relative humidity
1322 forcing has very high values (>80%) are highlighted in light green. The open symbol reflects a
1323 single site (CAZ) where simulated above ground biomass is very low. See supplementary online
1324 material for location and description of sites (Table S1). Pearson's correlation coefficient (*r*) and
1325 the significance level (***, P < 0.001) were calculated including all sites.
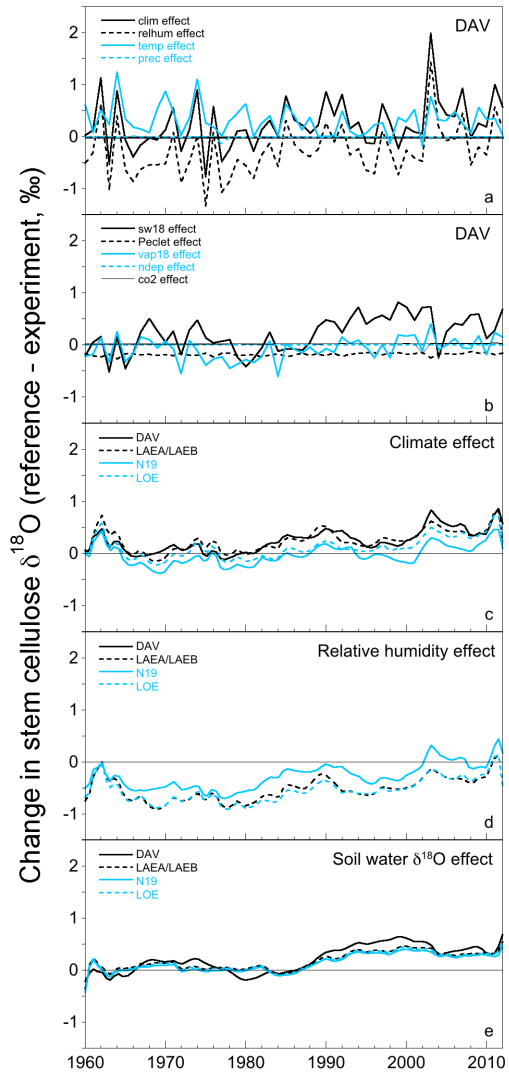
1326

1327

Figure 5. Comparison of measured (data) and simulated (model) stem cellulose δ^{18}O (panels a, h-k) for the alpine sites Davos (DAV), and Lötschen Valley (N19, LOE), and sites Lägern (LAEA, LAEB) in the Swiss Central Plateau. Standard errors (dashed lines) are based on measurements of ten trees. Panels b-f show input data as used for the simulation of stem cellulose δ^{18}O in LPX-Bern for site DAV (average of June, July, and August is presented). The vertical dashed line highlights the extremely hot summer 2003. Pearson's correlation coefficients, r, with simulated stem cellulose δ^{18}O are shown. Significance levels for the correlations are (*, P < 0.05; **, P < 0.01; ***, P < 0.001). Panels g and l-n show the ^{18}O-enrichment in stem cellulose above soil water δ^{18}O. Note that in LPX-Bern sites LAEA, LAEB, N19, and LOE lie within the same grid cell but are represented by different tree functional types (broad-leaved deciduous (LAEA, LAEB), needle-leaved evergreen (N19), and needle-leaved deciduous (LOE)).

Figure 6. Influence of forcing factors and the Péclet parameterization on simulated $\delta^{18}O$ of stem cellulose. Panels a and b show results for the alpine site in Davos (DAV) and for all factors investigated. Panels c, d, and e each show the influence of one individual, major driver for five sites, located within the Swiss Central Plateau (Lägeren (LAEA and LAEB, black, dashed line)), and the high-elevation sites in the Lötschen Valley (N19, blue, solid; LOE; blue, dashed) and in Davos (DAV, black solid). Each curve shows the differences in $\delta^{18}O$ of stem cellulose between the reference simulation (all forcings vary) and one sensitivity simulation (one forcing factor is kept constant). Constant forcing factors include relative humidity (relhum effect), air temperature (temp effect), precipitation (prec effect), soil water $\delta^{18}O$ (sw18 effect), water vapor $\delta^{18}O$ (vap18 effect), atmospheric nitrogen deposition (ndep effect), atmospheric CO_2 (co2 effect)) or a combination of constant forcings (climate (clim effect), i.e., temperature, precipitation, cloud cover, and number of wet days). An additional simulation is run without the Péclet effect (Peclet effect). The curves are smoothed with Stineman functions in panels c, d, and, e.
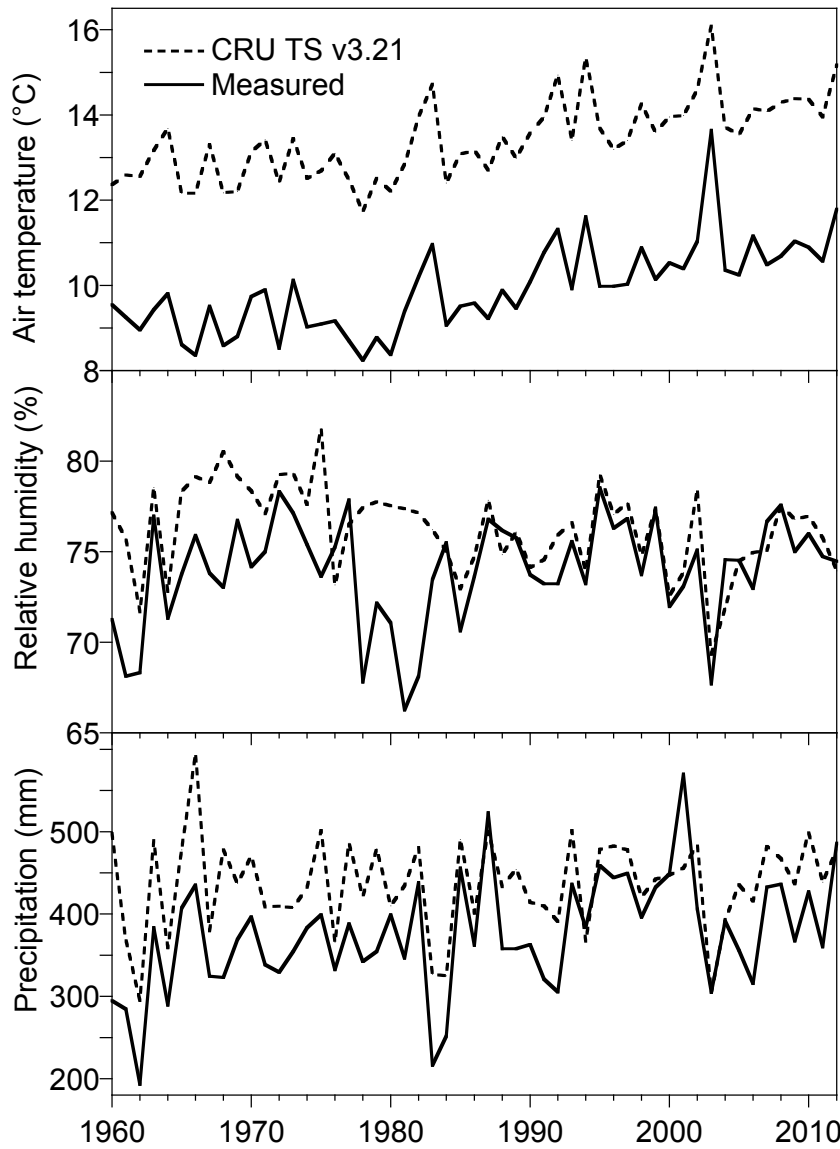
1389

1390

44

Figure 7. Comparison of climate input data for the alpine site Davos (DAV). Solid lines show grid cell average data from the CRU climatology (CRU TS v3.21) as used in our standard model setup. Dashed lines show data from a nearby meteorological station as used in a sensitivity simulation (run 'ewcTmeteo' in Fig. 8). Temperature is warmer and precipitation higher in the grid cell average data compared to the local data.
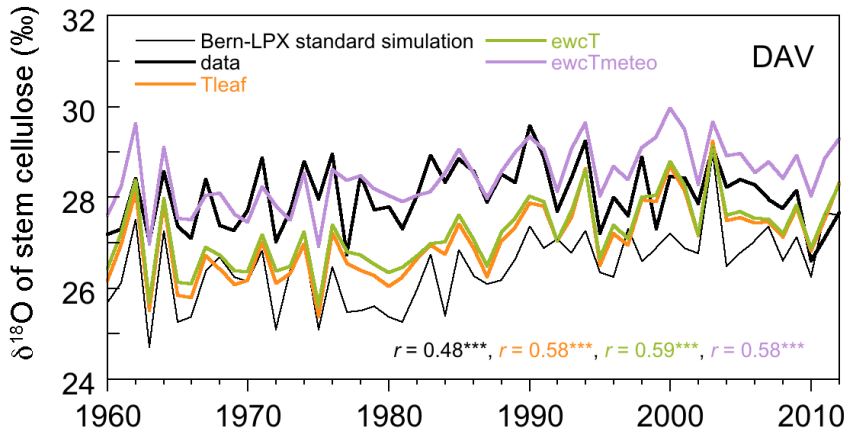
Figure 8. Effect of reduced leaf temperature and a temperature dependent biochemical fraction (ε_{wc}) on simulated stem cellulose $\delta^{18}O$ for site DAV (Davos). Leaf temperature was decreased by 3.5°C relative to air temperature ('Tleaf') because at site DAV, measured air temperature was on average 3.5°C lower than temperature from CRU TS v.3.21 used in the model ('LPX-Bern standard simulation'). The temperature dependent biochemical fraction was tested with the air temperature from CRU ('ewcT') and with measured air temperature from a nearby meteorological station ('ewcTmeteo'). Pearson's correlation coefficients, r, with measured stem cellulose $\delta^{18}O$ are shown. Significance levels for the correlations are (*, P < 0.05; **, P < 0.01; ***, P < 0.001).

Response to reviews

Anonymous Referee #1

1428 Received and published: 20 December 2015

1429 Motivated by paleo-climate/hydrological applications Keel et al. have implemented oxygen
1430 isotope diagnostics for tree ring cellulose in a dynamic vegetation model. They show that the
1431 model is able to reproduce measured modern-era oxygen isotope ratios of tree ring cellulose with
1432 a significant skill, and conclude that the model is a useful tool for paleo-interpretations of tree
1433 ring cellulose.

1434 In my view the manuscript would be suitable for publication with moderate revisions taking into
1435 account the following questions and comments.

1436 General comments. The paper is well written and the methodology is predominately well
1437 described with well-motivated choices for how the isotope diagnostics are imple- mented.

1438

1439 Thank you

1440

1441 Overall I think that structure and order of the figures related to the text could be improved, which
1442 would make manuscript easier to follow (see also detailed comments below).

1443

1444 We changed the order of figures and merged some as suggested below.

1445 Fig. 1: Soil water and vapor d18O

1446 Fig. 2: Leaf water d18O

1447 Fig. 3a: Leaf water 18O enrichment (previously Fig. 5)

1448 Fig. 3b: Stem cellulose d18O map (previously Fig. 6)

1449 Fig. 4: Scatter plot of simulated cellulose d18O vs. measurements (previously Fig. 7)

1450 Fig. 5a-g: Simulations/input data for site DVN (previously Fig. 8)

1451 Fig. 5h-k: Simulations for site LAB, LAA... (previously Fig. 4)

1452 Fig. 6: Sensitivity analysis (previously Fig. 9)

1453 Fig. 7: CRU vs. measured climate (previously Fig. 3)

1454 Fig. 8: Test with Tleaf and ewcT (previously Fig. 10)

1455

1456 Although I think that the comparison to data and validation of the model is generally well thought
1457 out, I miss a more thorough discussion/test of how chances in seasonality could affect the
1458 interpretation. E.g. how would the timing of spring melt affect results in high-latitude regions?
1459 How would changes in precipitation seasonality affect humidity limited regions? What are the
1460 implications of southern versus northern slope proximity of trees? These questions are
1461 particularly important for palaeoclimatic interpretation. I am aware that a full study would be

1462

1464

1465 We added:

1466 „In general, we expect any changes in seasonality that could potentially affect soil water d18O
1467 such as e.g. earlier snow melt to be translated to stem cellulose d18O in LPX."

1468

1469 In our sensitivity analysis precipitation (amounts) had no influence on stem cellulose d18O.
1470 Hence, it seems unlikely that LPX will capture changes in precipitation patterns that are not
1471 associated with changes in isotope signals.

1472 We added:

1473 "Hence, it seems unlikely that $\delta^{18}O$ as simulated by LPX-Bern will capture changes in
1474 precipitation patterns that are not associated with changes in isotope signals."

1475

1476 Sites LOE and N19 are in close proximity, but on a south- and north-facing slope respectively.
1477 The data presented in Fig. 4 show that LPX simulates nearly identical stem cellulose d18O that
1478 only differs because the PFTs are not the same.

1479

1480 Detailed comments.

1481 P18465, L2 Other references to millennial-scale tree ring isotope records include Edwards et al.
1482 2008.

1483

1484 Reference added

1485

1486 P18465, L18 For comparisons between variability of modelled and ice core d18O see Sjolte et al.
1487 2011 and Masson-Delmotte et al. 2015.

1488

1489 Reference added

1490

1491 P18468, L18 Replace "... carbon (C) and N dynamics..." with "... carbon (C) and nitrogen (N)
1492 dynamics..."

1493

1494 Changed

1495

1496 P18469, L12 Please clarify the choice of 0.8 for the ratio between the CO2 mole fraction in the

stomatal cavity and the ambient air.

Text modified to read: " for a fixed ratio, λ, between the CO2 mole fraction in the stomatal cavity and the ambient air. λ is set equal to 0.8 following Sitch et al. (2003) to approximate non-water-stressed conditions and as a starting value for the iterative computation of carbon assimilation and transpiration."

P18472, L24 Please clarify that this paragraph is an evaluation of the input data.

The following was added to begin the paragraph: "Next, the CRU climate input data are briefly evaluated."

P18473, L7-12 Optimally model output for daytime Rh should be applied. Variations in cloudiness etc. has large impacts on daytime Rh how valid is the 10% correction on longer time scales? E.g. decadal vs. intra-seasonal variations?

For a few summer days we compared average relative humidity for 24h vs. 08:00-18:00 and found that the reduction by 10% was sufficient. We added: 'This correction was evaluated for a few summer days at the site DVN and found to be sufficient'

P18477, L9 I think that especially the results section, and the paper in general, could benefit from grouping figures differently. I suggest grouping maps that are similar together as figures with several sub-panels with 2-4 panels per figure. At least figure 5 and 6 could easily be merged. Additionally, all sub-panels and sub-plots should be clearly marked with figure indices.

Figure 5 and 6 were merged and indices were added to subpanels. Similarly, figure 4 and 8 were merged.

P18478, L15 For the comparison with the measured data: is there a bias in the model elevation that could explain some of the discrepancy between model and data?

The following text was added: "We recall that LPX is run with a resolution of 3.75° x 2.5° which implies mismatches between local site conditions (altitude, climate, etc) and grid-cell averages as used to force the model. "

References

Thomas W.D. Edwards, S. Jean Birks, Brian H. Luckman, Glen M. MacDonald, Climatic and hydrologic variability during the past millennium in the eastern Rocky Mountains and northern

49

1534 Great Plains of western Canada, Quaternary Research, Volume 70, Issue 2, September 2008,
1535 Pages 188-197, ISSN 0033-5894, http://dx.doi.org/10.1016/j.yqres.2008.04.013.

1536

1537 Masson-Delmotte, V., Steen-Larsen, H. C., Ortega, P., Swingedouw, D.,
1538 Popp, T., Vinther, B. M., Oerter, H., Sveinbjornsdottir, A. E., Gudlaugsdottir,
1539 H., Box, J. E., Falourd, S., Fettweis, X., Gallée, H., Garnier, E., Gkinis,
1540 V., Jouzel, J., Landais, A., Minster, B., Paradis, N., Orsi, A., Risi, C.,
1541 Werner, M., and White, J. W. C.: Recent changes in north-west Greenland climate
1542 documented by NEEM shallow ice core data and simulations, and implications for past-
1543 temperature reconstructions, The Cryosphere, 9, 1481-1504, doi:10.5194/tc- 9-1481-2015, 2015.

1544

1545 Sjolte, J., G. Hoffmann, S. J. Johnsen, B. M. Vinther, V. Masson‐Delmotte, and C. Sturm
1546 (2011), Modeling the water isotopes in Greenland precipitation 1959–2001 with the meso‐
1547 Rscale model REMO‐iso, J. Geophys. Res., 116, D18105, doi:10.1029/2010JD015287.

1548

Anonymous Referee #2

Received and published: 18 January 2016

In this paper Keel and colleagues have implemented oxygen isotope signals (_18O) in soil and leaf water pools and wood cellulose in the global-scale land surface model LPX-Bern. This model is forced by monthly, gridded meteorological fields from the CRU for the period 1901-2010 and monthly, gridded isotope forcing provided by the coupled atmosphere-land surface model ECHAM5-JSBACH for the period 1960 to 2012. The LPX-Bern model is then ran at a daily timestep and tested against annually- resolved treering cellulose _18O dataset from field sites in Switzerland and 1960-2003 average tree- ring cellulose _18O data from sites across Europe. A sensitivity analysis of some relevant climate drivers or biophysical parameters is also performed.

In my opinion this paper is suitable for publication provided that the authors provide a bit more information on the model simulations and on how they draw some of the conclusions.

Thank you

Regarding the model simulations I could not see any information on how the monthly atmospheric forcing was used to run the LPX-Bern surface model at a daily time step.

Text was added in section 2.3 (page 18472, line 23 of the original MS): "The meteorological data are linearly interpolated to daily values, except for precipitation where a stochastic weather generator is applied to compute daily precipitation following Gerten et al. (2004)."

I was also surprised to see that daytime air relative humidity was assumed to be only 10

50

1572

Apparently, this sentence was incomplete. We noted in the text that relative humidity is downward corrected by an absolute value of 10%. Thus, we do not assume a relative humidity of 10%.

1576

Regarding the way some conclusions are drawn, I was missing some steps in several places. For example, on page 18479 lines 13-15, the authors claim that the model reproduce treering _18O across Europe "within the uncertainty of soil water _18O", but no statistical test is presented to support this statement, no value on the "uncertainty of soil water _18O" is given, and the single-site example given to support the statement (Table 1) shows that the soil water _18O is actually relatively well captured by the model while the biggest difference arise in the leaf water (and cellulose) _18O signal. To me this is a clear indication that biases in relative humidity (and leaf temperature) are more likely responsible for the differences found between observed and modelled tree ring _18O at this site. This is actually confirmed by the authors later on (e.g. page 18481 lines 14 and 18 or page 18482 line 9).

1587

It is not our intention to imply that uncertainty in soil water 18O data represent the largest uncertainty for simulated tree ring d18O values. To avoid confusion the statement was changed to read: "We conclude that LPX-Bern is able to represent the magnitude and the spatial climatological pattern of d18O in stem cellulose in Europe, generally within a few per mil of available observations.

1593

The conclusion drawn on page 18480 lines 27-29 seems also to lack some steps as it does not seem to follow logically from what is said just before.

This sentence on line 27-29 was moved to the end of the previous paragraph (line 14 of the original MS)

1598

I also found the the ordering of the figures is somehow confusing. I would not refer to figures in the material and methods if the figures are not commented there.

1601

We removed references to figures in the material & methods. The new order of figures has been described above.

1604

Other minor comments are given below:

1606

Page 18464

Line 4 "not been made use of" could be reformulated. Line 5 "could" has an ambiguous subject

1609

1610　Sentence on line 4/5 was changed to: "So far the use of stable oxygen isotope signatures of tree
1611　rings has not been systematically evaluated in dynamic global vegetation models (DGVMs).
1612　DGVMs integrate many hydrological and physiological processes and their application could
1613　improve proxy-model comparisons and the interpretation of oxygen isotope records."

1614

1615　Lines 7-10 "compare well" (twice) is a bit too vague

1616

1617　"well" on line 7 was replaced by "lie within a few permil". "well" on line 10 was deleted

1618

1619　Page 18465

1620　Line 4-5 It should be noted that this is a difficult task as cross-lab synthesis of _18O data can
1621　contain large biases. Do you have an idea of the bias on your particular dataset?

1622

1623　Most of the data used in our study are from the ISONET study for which an inter-laboratory
1624　comparison has been made: Boettger, T., et al. (2007). For d18O in cellulose the variation
1625　reached 0.58 permil for the means.

1626

1627　Line 20 Hyphen should be removed.

1628

1629　Done.

1630

1631　Page 18466

1632　Line 13 The term "boundary conditions" can be misleading as it suggests that the LPX-Bern
1633　model is ran/used only on a limited domain, rather than at the global scale. Maybe use the term
1634　"isotopic forcing"?

1635

1636　Term replaced by "used as oxygen isotope input data (i.e. isotope forcing)."

1637

1638　Also is it realistic to use CRU meteorological data together with ECHAM _18O data, e.g. if CRU
1639　and ECHAM5 precipitation do not coincide? I guest at a monthly timescale it is not of an issue
1640　but maybe at some locations during the dry season.

1641

1642　We are not aware of any data product that provides an observation-based evolution of soil water
1643　d18O during the past 50 years. Thus, we have to rely on the ECHAM data. Haese et al. (2013)
1644　estimate that the root mean square error between precipitation d18O simulated by ECHAM5-
1645　JSBACH and the GNIP data is 1.78 ‰.

Sentence modified to read: "The $\delta^{18}O$ of surface soil water reflects the $d^{18}O$ signal of precipitation averaged over a certain amount of time and is further modified by evaporation of soil water leading to evaporative enrichment and potentially by mixing with ground water."

Statement modified to read: "This Péclet effect tends to reduce the signal of evaporative enrichment in bulk leaf water and the effect is large when transpiration rates are high."

Done.

We added an explanation for bulk leaf water (i.e. whole leaf water):

Text changed to read: "but additional processes related to d18O signals in leaf water and stem cellulose are resolved at varying degrees of complexity"

Text on line 10 amended by: ".. and as we lack detailed species-specific information, e.g. on water flow and the Péclet effect."

53

1681

Line 2 Does it mean that you have multiple PFTs sharing the same soil and space, i.e.,competing for light as well?

We now specify: 'Light competition is modeled indirectly by assigning a higher mortality to PFTs with a small increment in fractional plant cover and biomass compared to PFTs with a large increment (Sitch et al., 2003).'

Line 5 Is this maximum transpiration equal to potential ET?

No. Esupply is the maximum transport rate of water from the soil to the leaves. Text clarified to read

"Esupply is the product of root-weighted soil moisture availability and a maximum water supply rate that is equal for all PFTs (Sitch et al., 2003)."

Line 9 Are gm and _m species-specific parameters?

We made this clear by adding:

"that are equal for all plant functional types".

Line 12 Why is the ratio of intercellular to ambiant CO_2 mixing ratio set to 0.8? It is very high no?

See above

Line 17 I would reformulate "which is a Farquhar model".

We reformulated this: "Photosynthesis is modeled following (Collatz et al., 1991, 1992), which is based on the formulation by Farquhar et al. (1980) and Farquhar and von Caemmerer (1982) generalized for global modeling purposes."

Line 21 Does it mean the model is using a daily time step? It has not been stated so far.

Text added on p. 18468 and line 23: ".. Wania et a., 2009), and features a daily time step for photosynthesis and evapotranspiration."

54

1716

Line 2 I guess _ is the same parameter that is set to 0.8 in the previous paragraph. Maybe introduce the symbol before?

Done.

Line 8 I think Farquhar and Lloyd (1993) is a better reference.

We replaced this reference by Farquhar and Lloyd (1993)

Line 19 Why using such a high value (32‰). This is the upper bound in the literature and it is quite controversial.

We chose the value based on an experimental assessment by Cappa et al. 2003 and added the reference.

Line 6 Does this value of L comes from Faruhar and Lloyd (1993)? Why is it not PFT specific? Maybr cite Kahmen et al. (2009) here?

The formulation is indeed misleading and was changed as follows:

"... the dilution of 18O-enriched leaf water... is effective over a path length L (Farquhar and Lloyd, 1993). To keep the model as simple as possible we set L to 0.03 m for all PFTs following (Kahmen et al. 2011), although L can vary largely between species (Kahmen et al. 2009)."

Equation 6 Do you have a reference? It seems to come from Cuntz et al. (2007) but there is a typo there. Maybe use a different formulation that has no typo (e.g. Braud et al. 2005 Eq. C1 or Cuntz et al. 2007 Eq. A23) or mention original Eq. A22 but state there is a typo?

We added the reference Cuntz et al. (2007) and mention that there is a typo in equation A22 that we use.

Line 13 Rather than "high transpiration rates" I would say "low relative humidity" or "highevaporative demand".

1750

55

1751 We prefer to keep the wording because it is indeed the leaf transpiration rate that determines the
1752 Peclet effect as evident from the equations given in the text.

1753

1754

1755 Line 1 You cite Sternberg et al. (1986) above. Why about results from Sternberg and Vendramini
1756 (2001) (see their Figure 1)?

1757

1758 We could not find the publication by Sternberg and Vendramini (2001).

1759

1760 Line 8 "with a daily time step": finally. . .

1761

1762

1763 Line 7-12 This reduction in relative humidity between daytime and daily values seems rather low.
1764 How large is the reduction in the data from Meteoswiss? Also it is stated before that the output
1765 data from ECHAM5-JSBACH are at monthly time scale. How do you go to the daily time scale
1766 from then?

1767

1768 See comment above

1769

1770 Line 16-17 How is the _18O of soil water in JSBACH used in the soil water scheme of LPX
1771 given that the soil vertical discretisation seems quite different? You would need to provide
1772 explanations for this important aspect. Also how is the soil evaporative enrichment treated in
1773 LPX?

1774

1775 We added: "In ECHAM5, there are no soil layers and the isotopic composition has no vertical
1776 gradient. Any water taken up by plants has the d18O of soil water. The soil layers in LPX do not
1777 affect the isotopic composition, but are exclusively used for quantitative assessment of water
1778 pools and fluxes."

1779

1780 In ECHAM5 the evaporative enrichment is affected by an equilibrium and a kinetic fractionation
1781 factor as described in more detail in Haese et al. (2013).

1782

1783

1784

1785 Line 23-25 But Tair is already 4_C higher than the observed no?

1786

1787 Yes, Tair is indeed already about 4 degree C higher. We reran the simulation and reduced the leaf
1788 temperature by 3.5 degree, because on average measured air temperature at site DVN is 3.5 lower
1789 compared to CRU temperature used in LPX-Bern. The text was modified accordingly.

1790

1791 And what about the other terms that depend on leaf temperature, including the relative humidity
1792 term?

1793

1794 For this simple test we did not change any other terms and we added: 'while all other terms
1795 remained unchanged.'

1796

1797 Page 18475 Line 11-13 Not very clear from this figure.

1798

1799 We added: 'model time series shown in Figure 5...(..thin lines in Fig. 5)'

1800

1801 Page 18477 Line 2 The order of the figures is a bit strange. I would not introduce them in the
1802 material and method section if not commented there.

1803

1804 We changed the order of figures as described above.

1805

1806 Page 18479 Line 10 30gC/m2 is extremely low. Are you sure of the units? Aso _18O of which
1807 pool are we talking about here?

1808

1809 The above ground biomass at this site is indeed very low as this grid cell is dominated by
1810 herbaceous plants. This is why we exclude it. We made this more clear:
1811 'extremely low biomass ..., because herbaceous plants dominate in this grid cell' We added:
1812 'stem cellulose d18O" to make clear which pool we refer to.

1813

1814 Line 11 I guess "these" refer to the humid sites + CAZ but should be stated a bit more clearly
1815 maybe.

1816

1817 Was changed

1818

1819 Page 18480 Line 24 Not clear from figure. Maybe draw a line fo 2003?

1820

1821 Line was added to highlight year 2003.

1822

1824

1825   We added: ', e.g. the effect of soil water d18O varied around zero in the 1960s and is consistently
1826   positive in the 1990s (Fig. 9b).'

1827

1829

1830   We added Haese et al. (2013).

1831
1832
1833